The role of glutathione depletion in skeletal muscle apoptotic signalling in young and old rats

by

Crystal Lalonde

A thesis
presented to the University of Waterloo
in fulfillment of the
thesis requirement for the degree of
Master of Science
in
Kinesiology

Waterloo, Ontario, Canada, 2010

AUTHOR'S DECLARATION

I hereby declare that I am the sole author of this thesis. This is a true copy of the thesis, including any required final revisions, as accepted by my examiners.

I understand that my thesis may be made electronically available to the public.

ABSTRACT

There is substantial evidence that oxidative stress causes negative outcomes in many cell and tissue types. This is especially true of skeletal muscle, as it is continually subjected to various sources of reactive oxygen species (ROS). Oxidative stress in muscle has been linked to several disease states as well as to the normal aging process. Oxidative stress has also been associated with increased apoptotic signalling. Furthermore, elevated apoptosis is consistently observed in aged skeletal muscle and is thought to be one of the mechanisms of age-related muscle atrophy. Due to its post-mitotic nature, skeletal muscle may be more susceptible to the harmful effects of oxidative stress in light of its limited regenerative capacity. As a protective measure, a sophisticated antioxidant system exists in muscle consisting of both enzymatic (superoxide dismutases (SOD's), catalase, glutathione peroxidase) and non-enzymatic elements (glutathione: GSH). GSH is a ubiquitously expressed tripeptide essential to maintenance of the redox status of the cell. Its role in skeletal muscle apoptosis, especially in different muscle types, is currently unclear. To elucidate the potential role of GSH in skeletal muscle apoptosis and oxidative stress, L-buthionine-[S,R]-sulfoximine (BSO) was used to deplete GSH in young (34.85 ± 0.68 wks) and old (69.11 ± 3.61 wks) male Sprague-Dawley rats. Thiol levels (GSH, GSSG), ROS production, 4-hydroxy-2-nonenal (4HNE) levels, DNA fragmentation and apoptosis-related protein expression were examined in soleus (SOL) and white gastrocnemius (WG) muscle. BSO led to significant GSH depletion (89% in SOL, 96% in WG) compared to age-matched controls. Catalase upregulation, in the absence of change in SOD levels, was evident as a result of BSO treatment and advancing age in both muscle tissues. BSO treatment also resulted in increased DNA fragmentation in WG and SOL, with elevated ROS production in SOL only; both of these effects were independent of age. Advancing age resulted in elevated caspase activity and Hsp70

protein content, with a concomitant decrease in anti-apoptotic ARC in SOL but not WG. Additionally, ROS production, 4HNE content, DNA fragmentation and ARC levels were all significantly elevated in SOL compared to WG. These data indicate that SOL may be subjected to a state of elevated cellular stress. There is also some evidence that GSH depletion increases DNA fragmentation while age contributes to a degradative loss of glycolytic muscle.

ACKNOWLEDGEMENTS

I would like to take this opportunity to thank the people in my life who have contributed to the successful completion of this master's thesis. First and foremost, my thesis advisor Dr. Joe Quadrilatero: thank you for always pushing me to excel and challenging me, even when all I wanted was a simple answer. Your mentorship and balance of serious work ethic and fun times have truly been an inspiration to me. I doubt I will ever have another supervisor like you; you truly are one in a million JQ. I would also like to sincerely thank my committee members, Drs. James Rush and Marina Mourtzakis, for providing me with helpful feedback, for making time for all of my questions, and for offering encouragement when the science was just not going as planned. A really big thank you goes out to Dr. James Rush, Steven Denniss and Andrew Levy for all of their work in establishing the BSO model. Additional thanks to Steve and Lev for caring for the animals throughout the entire tissue collection period. My thesis would not have been possible without their help and diligence in animal care.

Of course, huge thanks go out to the members of the Muscle Biology and Apoptosis Laboratory; Aaron Dam, Elliott McMillan, Darin Bloemberg and Andrew Mitchell. You guys have made graduate school truly memorable: from late nights in the lab working out the Xience to all of our extracurricular shenanigans, you've all been amazing supports and awesome friends. The various undergraduate students in our lab who helped with sample prep and tube labelling also deserve thanks, since my work would have taken much longer without their help!

Last but not least, I need to thank my family (aka my mom) and my close friends. Mom, you have always been my biggest supporter. Even though more school is on the horizon, I'm so grateful for everything you've done for me so far in helping me get to where I am today. And to

my close friends, thank you so much for being shoulders to cry on, for making me laugh when I needed it, and for keeping me sane when I thought school would never end. I could never have done it without you.

TABLE OF CONTENTS

LIST OF FIGURES

LIST OF ABBREVIATIONS

(*In order of appearance in-text*)

HIV: Human Immunodefiency Virus

AIDS: Acquired Immuno Deficiency Syndrome

DNA: Deoxyribonucleic Nucleic Acid

CD95 (Fas): Cluster of Differentiation 95

TNFR1: TNF Receptor 1

TRAIL: TNF-Related Apoptosis-Inducing Ligand

FasL: Fas Ligand

TNFα: Tumour Necrosis Factor alpha

FADD: Fas-Associated Death Domain

TRADD: TNF Receptor-Associated Death Domain

DISC: Death-Inducing Signalling Complex

DED: Death Effector Domains

AIF: Apoptosis-Inducing Factor

Smac: Second Mitochondrial Activator of Caspases

Bcl-2: B-Cell Lymphoma-2

Bax: Bcl-2-Associated X protein

Bak: Bcl-2 homologous Antagonist/Killer

Bok: Bcl-2 associated Ovarian Killer

Bid: Bcl-2 Interacting Domain

Bcl-xL: B-Cell Lymphoma-extra large

APAF-1: Apoptotic Protease-Activating Factor-1

ATP: Adenosine TrisPhosphate

IAP: Inhibitor of Apoptosis Protein

tBid: Truncated BH3-Interacting Death domain agonist

EndoG: Endonuclease G

NADH: Nicotinamide Adenine Dinucleotide

RNA: RiboNucleic Acid

FLIP: FLICE-like Inhibitory Protein

ARC: Apoptosis Repressor with Caspase recruitment domain

EDL: Extensor Digitorum Longus

Hsp70: Heat Shock Protein-70

ROS: Reactive Oxygen Species

H_2O_2: Hydrogen Peroxide

$O_2^{\cdot -}$: Superoxide Anion

$OH^{\cdot}$: Hydroxyl Radical

OH^-: Hydroxyl Anion

MnSOD (*Sod2*): Manganese SuperOxide Dismutase

MAPK: Mitogen-Activated Protein Kinase

NFκB: Nuclear Factor KappaB

PGC-1α: Peroxisome proliferator-activated receptor-gamma coactivator-1alpha

NADPH: Nicotinamide Adenine Dinucleotide Phosphate

XO: Xanthine Oxidase

NADH: Nicotinamide Adenine Dinucleotide

TUNEL: Terminal deoxynucleotidyl transferase dUTP Nick End Labeling

4-HNE: 4-hydroxy-2,3-nonenal

8-OHdG: 8-hydroxydeoxyguanosine

GSH: reduced Glutathione

SOD: SuperOxide Dismutase

mRNA: messenger RNA

CuZnSOD: Cu/Zn-containing SuperOxide Dismutase

γ-GCS: gamma-Glutamylcysteine Synthetase; also known as Glutamate-L-Cysteine Ligase

GSSG: Glutathione Disulfide or oxidized Glutathione

GPx: Glutathione Peroxidase

GR: GSSG Reductase

BSO: L-buthionine-[S,R]-sulfoximine

APO-1: antibody raised against an antigen identical to Fas

BA: Bongkrekic Acid

ANT: Adenine Nucleotide Transporter

MPT: Mitochondrial Permeability Transition

NAC: N-AcetylCysteine

HEPES: 4-(2-HydroxyEthyl)-1-PiperazineEthaneSulfonic acid

NaCl: Sodium Chloride

$MgCl_2$: Magnesium Chloride

DTT: DiThioThreitol

BCA: BiCinchoninic Acid

KCl: Potassium Chloride

EDTA: EthyleneDiamineTetraAcetic acid

EGTA: Ethylene Glycol TetraAcetic acid

SDS-PAGE: Sodium Dodecyl Sulfate-PolyAcrylamide Gel Electrophoresis

PVDF: PolyVinyliDene Fluoride

TBS-T: Tris-Buffered Saline + Tween

HRP: HorseRadish Peroxidase

ECL: Enhanced ChemiLuminescence

AU: Arbitrary Units

HPLC: High Performance Liquid Chromatography

$NaHCO_2$: Sodium Hydrogen Carbonate

DCFH-DA: 2’7’DiChloroHydroFluorescein DiAcetate

PBS: Phosphate-Buffered Saline

LIST OF PRINCIPAL APOPTOTIC FACTORS AND FUNCTIONS

Caspase-3: terminal effector caspase, cleaves poly-ADP-ribose polymerase (PARP) leading to DNA fragmentation. Also leads to cleavage of caspase-dependent DNase that contributes to DNA fragmentation.

Caspase-8: initiator caspase, primarily in the extrinsic apoptotic pathway. Also participates in the intrinsic, mitochondrial pathway by cleaving pro-apoptotic Bid.

Caspase-9: initiator caspase, primarily in the intrinsic apoptotic pathway; proteolytically activated by the formation of the apoptosome, consisting of procaspase-9, cytochrome c, deoxyATP, Apaf-1.

Caspase-2: this caspase's mechanism of activation is presently unclear, but it is proposed to play a role in mitochondrial-mediated cell death or to direct cause cell death upon activation.

Caspase-12: protease released from the endoplasmic reticulum that leads to downstream cleavage of the effector caspase-3.

TNF-α: death ligand/activator of the extrinsic apoptotic pathway

Fas (CD95): death ligand/activator of the extrinsic apoptotic pathway.

AIF: involved in caspase-independent cell death; translocates to the nucleus upon release from mitochondria, leading to DNA fragmentation.

Bcl-2 (Bcl-x_L): anti-apoptotic members of the Bcl-2 family of proteins; inhibit mitochondrial pore formation through interaction with pro-apoptotic Bcl-2 family members (ie. Bax, Bid).

Cytochrome c: component of the mitochondrial electron transport chain, released into the cytosol upon apoptotic stimulus to participate in caspase-9 activation through formation of the apoptosome.

Smac: Pro-apoptotic mitochondrial factor, released from the mitochondrial intermembrane space upon apoptotic stimulation. It then interacts with Inhibitor of Apoptosis Proteins (IAPs) to activate the caspase cascade.

Bax (Bak, Bok): pro-apoptotic Bcl-2 family members, translocates to and inserts into the mitochondria outer membrane upon apoptotic stimulation, leading to pore formation and loss of mitochondrial membrane potential.

Bid: small pro-apoptotic Bcl-2 family member, must be cleaved by caspase-8 to exert its pro-apoptotic action. Once activated, it interacts with Bax, contributing to mitochondrial outer membrane pore formation.

INTRODUCTION

Apoptosis is a tightly regulated, highly ordered mode of cell death also referred to as programmed cell death.[1] This process occurs through a series of cellular events that aid in the removal of unnecessary or damaged cells from an organism. For example, during embryogenesis, apoptosis of skin cells occurs between the digits of the hand which allows for the proper formation of the fingers.[2] Apoptosis is also implicated in several disease states, such as HIV/AIDS where widespread T cell-specific apoptosis occurs,[3, 4] cardiovascular diseases where apoptosis can be altered in several tissues such as heart, [5, 6] blood vessels[7, 8] and skeletal muscle,[9] and cancer where decreased apoptotic cell death prolongs malignant cell survival. [4, 10, 11, 12]

The hallmark morphological features of apoptosis include cell shrinkage, chromatin condensation, membrane blebbing, and formation of apoptotic bodies.[13] Apoptosis is a type of cell death that causes little damage to the surrounding cellular environment, unlike what is commonly observed when cells die by necrosis.[1] Along with organelle swelling, loss of membrane integrity and cell lysis, this latter form of cellular demise involves a large inflammatory response at the site of injury.[14] This leads to further damage or death of surrounding cells by initiating an exaggerated immune response, an event not typically observed during apoptotic cell death.[1] While mention of necrosis is important to the concept of cell death, the remainder of this thesis will focus on apoptotic cell death, with particular emphasis on its occurrence in skeletal muscle.

Caspases as the "executioners" of apoptosis

A defining point of the apoptotic death program is the reliance on a family of specialized proteolytic enzymes to bring about cell death. Caspases, or cysteine-aspartate proteases, are enzymes that cleave target proteins between cysteine and aspartic acid residues.[15] These enzymes can be divided into two groups, namely the initiator caspases, with the principal members consisting of caspases-8 and -9, whose activation leads to subsequent cleavage and activation of effector, or terminal, caspases such as caspases-3, -6, -7.[16] Caspases can cleave other downstream proteases or can activate effector enzymes that play a role in DNA fragmentation (ie. caspase-dependent DNAse).[17, 18] Caspase activation is both selective and very specific in that only certain signals initiate caspase signalling cascades, and only certain caspases will be activated depending on the nature of a particular signal. For example, binding of specific death ligands to their extracellular receptors, as seen in the extrinsic apoptotic pathway, preferentially activates caspase-8, which then transduces the death signal culminating in eventual cell death.[19, 20] The death signal is propagated by caspases through their ability to cleave other caspase zymogens, or procaspases located downstream in the signalling cascade, as seen with caspase-8-mediated caspase-3 cleavage.[19, 20] Additionally, certain caspases also undergo activation through oligomerization-induced autoproteolysis as observed with caspase-8[21, 22] and caspase-2 activation.[23]

The extrinsic apoptotic pathway

There are several pathways through which apoptosis can occur. In the extrinsic pathway (Figure 1; left side), specialized cell-surface receptors, or death receptors, are stimulated with their specific death ligand, leading to intracellular death signal propagation.[24] Common death

receptors include Fas or CD95, Tumour Necrosis Factor Receptor 1 (TNFR1), and TNF Related Apoptosis-Inducing Ligand (TRAIL) Receptors 1 and 2, with their associated death ligands, Fas ligand, TNF-α and TRAIL.[24] Upon appropriate ligand binding, death domains found on the intracellular portion of the death receptors are activated; these include Fas-associated death domain (FADD)[25, 26] or TNFR-associated death domain (TRADD).[27] Death domain activation leads to assembly of the death-inducing signalling complex (DISC).[28, 29] One of the components of the DISC is procaspase-8, a zymogen activated by proximity-induced oligomerization with the death effector domains (DED) belonging to FADD.[21, 22] Upon DISC assembly, the mature, initiator form of caspase-8 is released.[21, 30] Caspase-8 proteolytically cleaves cytosolic procaspase-3 to its active effector, caspase-3.[19, 20] This latter enzyme is responsible for large-scale cellular proteolysis and DNA fragmentation[17, 18] and is one of the principal convergence points for the extrinsic and intrinsic apoptotic pathways.

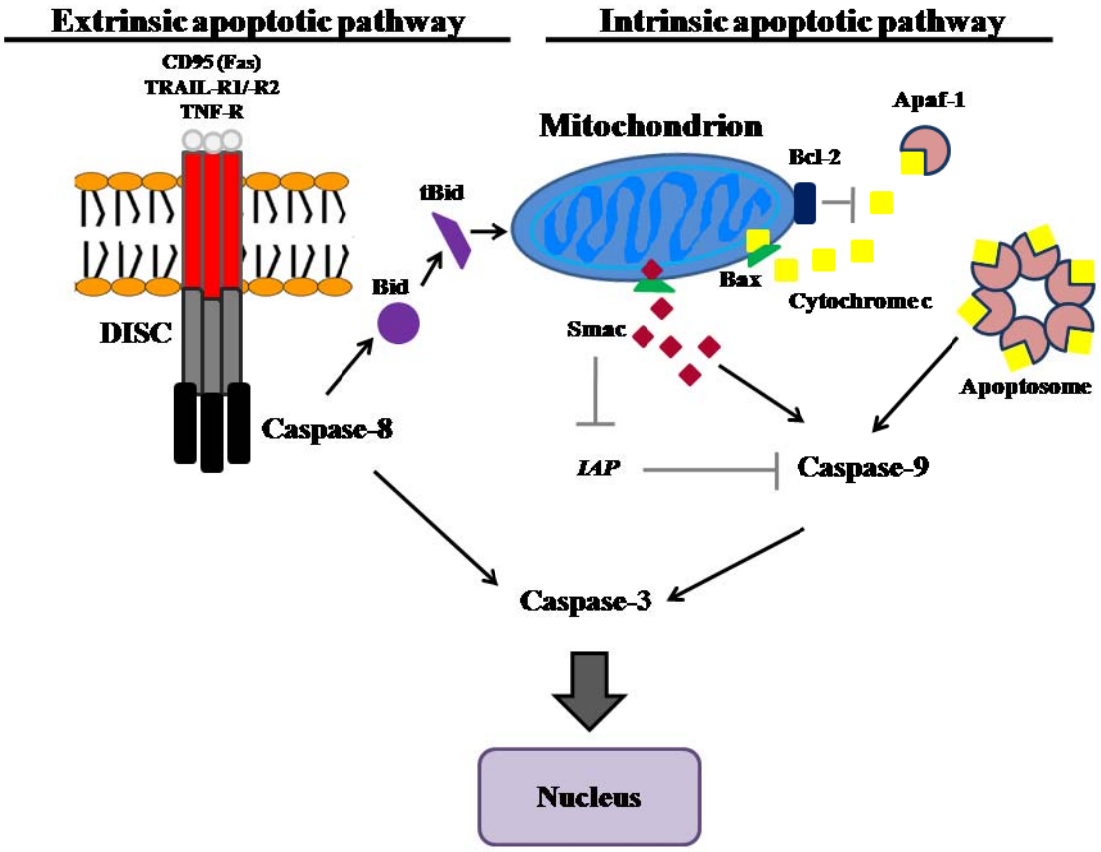

Figure 1: Simplified schematic of the extrinsic and intrinsic apoptotic pathways.

The intrinsic pathway

The intrinsic pathway (Figure 1; right side) centers on the mitochondrion and its release of a number of pro-apoptotic factors (ie. cytochrome c[31], Apoptosis Inducing Factor (AIF)[32], second mitochondrial activator of caspases (Smac)[33]) as a result of cellular stress. The release of these apoptogenic factors from the mitochondria is heavily dependent on the balance of pro- and anti-apoptotic members of the Bcl-2 superfamily of proteins, which are divided into 3 groupings based on commonly observed homologous protein domains (or BH domains). The pro-apoptotic members consist of the Bax subfamily which contains BH1, BH2 and BH3 domains and includes Bax, Bak and Bok, while the other "killer" proteins contain only the

BH3 domain (ie. Bid).[34] On the other hand, the anti-apoptotic members are part of the Bcl-2 subfamily and contain at least BH1 and BH2, with some members containing all 4 BH domains (ie. Bcl-2, Bcl-x_L).[34] The distribution of these BH domains is significant when considering the ways in which these proteins interact during apoptotic cell death. The BH3 domain is an essential component in both the anti-apoptotic and pro-apoptotic dimerizations that occur during Bax-Bcl-2 or Bax-Bax interactions, respectively.[35]

In most biological systems, pro-apoptotic Bax and anti-apoptotic Bcl-2 are the primary Bcl-2 family members of interest, as their opposing effects on mitochondria are so intimately tied to cell survival.[35, 36, 37, 38, 39] The balance between these proteins, the Bax:Bcl-2 ratio, is a frequently used measure of a cell's susceptibility to apoptotic cell death[40] , given the pivotal role of the Bcl-2 family members in regulating cell death.[35, 37, 38, 39] In terms of its pro-apoptotic role, Bax is primarily localized in the cytosol in healthy cells but translocates to the mitochondria as a result of an apoptotic stimulus and is inserted into the outer mitochondrial membrane. This leads to pore formation, also known as the mitochondrial permeability transition,[39, 41] subsequent loss of membrane potential and release of mitochondrial apoptosis-related factors.[31, 32, 33] Bcl-2 inhibits mitochondrial pore formation by heterodimerization with Bax at the mitochondrial outer membrane, thus preventing or at very least delaying release of apoptotic factors.[35]

When the apoptotic balance is shifted towards mitochondrial pore formation or membrane disruption, pro-apoptotic factors can be released into the cytosol which initiates apoptosis through distinct mechanisms. For example, cytochrome c can be released from the mitochondria[31, 39] and binds with Apoptotic Protease-Activating Factor-1 (Apaf-1), procaspase-9 and 2-deoxy-ATP in the cytosol.[42, 43] This results in the formation of the

apoptosome, and is a necessary component in self-cleavage and activation of procaspase-9.[42, 43] Caspase-9 can then cleave procaspase-3, permitting large-scale proteolysis in the cell.[17, 18] In addition, pore formation permits release of other apoptogenic proteins, such as Smac, which can indirectly activate caspases by inhibiting the action of a set of caspase inhibitors known as the Inhibitor of Apoptosis Proteins (IAPs).[33]

Lastly, there is evidence that both the intrinsic and extrinsic pathways may converge during apoptotic signalling.[44] In this sequence of events, activation of the intrinsic apoptotic machinery leads to caspase-8-mediated cleavage of the Bcl-2 family member Bid (Figure 1).[44] This pro-apoptotic factor is found in the cytosol and upon truncation by caspase-8, inserts into the outer mitochondrial membrane and contributes to pore formation and release of apoptogenic factors.[37]

Caspase-independent and calcium-mediated apoptosis

Apoptotic cell death can also be caused by two additional pathways. The first of these is the caspase-independent mitochondria-mediated pathway, which involves the release of the pro-apoptotic proteins Apoptosis-Inducing Factor (AIF)[32] and Endonuclease G (Endo G)[45]) from mitochondria. AIF is a flavenoid protein normally located in the mitochondria intermembrane space that possesses both electron acceptor/donor characteristics typical of NADH oxidases in addition to a death effector role.[46] Upon exposure to apoptotic stimuli, AIF is released into the cytosol, where it then translocates to the nucleus to cause chromatin condensation and large-scale DNA fragmentation.[32, 47, 48] Endo G is a nuclease located in the mitochondria, where its role is to produce RNA primers for DNA polymerase gamma.[49] However, apoptotic stimuli can

induce EndoG release from the mitochondria and subsequent translocation to the nucleus where, similar to AIF, it induces large-scale DNA fragmentation.[45]

Another series of events culminating in apoptotic cell death is the calcium-dependent calpain-mediated pathway. In this particular case, the calcium-dependent proteases calpains are activated by increased intracellular calcium concentrations[50], which activate caspase-12 released from the endoplasmic reticulum, leading to downstream activation of caspase-3.[51]

Apoptosis in skeletal muscle

The apoptotic pathways and molecules reviewed above are biologically conserved and are similar in many cellular systems, though the intricacies of the pathways may vary slightly depending on the tissue. A special case is skeletal muscle, which possesses some unique features with respect to apoptotic signalling and cell death. In most systems, an entire cell is typically removed when apoptosis is triggered.[4, 10, 52, 53, 54] However, due to the multi-nucleated nature of skeletal muscle, it can undergo a process known as myonuclear apoptosis, whereby only certain individual nuclei and their associated cytoplasmic portions are lost (Figure 2).[55, 56] This restricted loss is speculated, in the short term, to allow for preservation of muscle fiber integrity, resulting in maintenance of overall fiber number. However, this loss of nuclei would result in fiber and muscle atrophy through loss of that associated cytoplasmic portion, or myonuclear domain, of individual myonuclei.[55] Work conducted in rodent models of muscle atrophy, including hindlimb unloading[57, 58] and spaceflight,[59] has demonstrated decreased myonuclear number concomitant with a decreased myonuclear domain, events which are believed to be a primary cause of muscle fiber atrophy.[55, 60] The post-mitotic nature of skeletal muscle does not allow for typical regeneration, making the presence of satellite cells

essential to maintenance of muscle fiber integrity. Satellite cells are specialized progenitor cells found between the sarcolemma and the basement membrane of myocytes that can form myonuclei or entire muscle fibers to aid in muscle maintenance; however this regenerative capacity is limited.[50, 61]

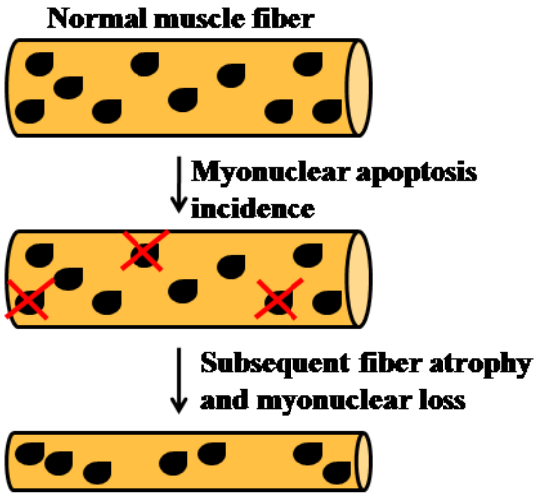

Figure 2: Simplified schematic of myonuclear apoptosis of skeletal muscle fibers.

Another distinctive characteristic of skeletal muscle with respect to apoptosis is the restricted expression of general apoptosis-related proteins.[62, 63, 64] For example, FLICE-like inhibitor protein (FLIP), an inhibitor of the extrinsic apoptotic pathway, has been shown to be highly expressed in skeletal muscle,[63] especially as a result of aging.[64] Another of these proteins, the apoptosis repressor with caspase recruitment domain (ARC), is also primarily found in post-mitotic tissues such as heart and skeletal muscle.[62] In addition to its unique tissue expression pattern, ARC is set apart from all other known apoptotic inhibitors by its ability to block both the intrinsic and extrinsic apoptotic pathways.[65] In particular, ARC interacts and oligomerizes with Bax through its caspase recruitment domain, thus inhibiting translocation of

Bax to the mitochondria.[65, 66] ARC also interacts with Fas and FADD, impairing death receptor activation, DISC assembly and subsequent caspase-8 activation.[62, 65]

Lastly, skeletal muscle is made up of several fiber types that vary in their metabolic characteristics, contractile properties, morphology, and mitochondrial content.[67, 68] For example, soleus is composed mainly of type I, or slow-twitch fibers and has a high oxidative capacity due to its elevated mitochondrial content. In contrast, extensor digitorum longus (EDL) is a glycolytic, fast-twitch muscle composed mainly of type IIB fibers with lower mitochondrial content.[68, 69] Given the importance of mitochondria in apoptosis, fiber type differences or alteration in mitochondrial content may influence apoptotic signalling. Therefore, differences in apoptotic signalling and expression may occur across different muscle fibers.

There is evidence of differential apoptotic signalling in fast and slow muscles, which adds another level of complexity to understanding the mechanisms of skeletal muscle apoptosis. For example, previous work has shown that the expression of ARC is differentially expressed in different fibers.[70] Recent work in our lab has shown that the expression of apoptosis-related proteins, such as AIF, Smac, cytochrome c, Hsp70, ARC and Bcl-2, is increased in slow, more oxidative muscle fiber types. In addition to these protein expression differences, caspase-3, -8, and -9 activity, as well as basal levels of DNA fragmentation are higher in red portions of the gastrocnemius versus white portions of this same muscle (McMillan & Quadrilatero, 2010). There is also some evidence of selective apoptosis or apoptotic signalling in specific muscles of a particular fiber type in aging.[71, 72, 73] For instance, Bax and caspase-3 content have been shown to be increased in EDL, but not soleus, with advancing age in rats.[73] TNF-α signalling is significantly elevated in superficial vastus lateralis

(predominantly type II muscle) compared to soleus muscle of old rats.[72] Although evidence of differential apoptosis or apoptotic signals in particular fiber types exists, further research is needed to better define apoptotic signalling in different types of skeletal muscle during aging and other disease states.

Cellular effects of oxidative stress

Oxidative stress occurs due to an imbalance between cellular oxidants or reactive oxygen species (ROS) and antioxidants, favouring higher oxidant concentration or production.[74] Some common cellular oxidants include hydrogen peroxide (H_2O_2), superoxide anion ($O_2^{\cdot -}$), hydroxyl radical ($OH^{\cdot}$), and hydroxyl anion (OH^-).[75] While an increased proportion of oxidants can be damaging in the long run, ROS production plays an essential role in cell signal transduction and adaptation. For example, the activity of antioxidant enzymes, such as MnSOD[76, 77] and catalase, [78] is upregulated in response to increased ROS production in skeletal muscle. In fact, inhibition of intracellular ROS production prevents activation of the MAPK/NF-κB signalling pathway in muscle that is primarily responsible for the above-mentioned upregulations.[79] Furthermore, recent work suggests that expression of peroxisome proliferator-activated receptor-γ coactivator-1α (PGC-1α), a powerful inducer of mitochondrial biogenesis, is increased 5.6-fold in rodent vastus lateralis muscle due to exhaustive exercise and associated ROS production.[80]

While ROS mediate positive signalling events, they can also result in more oxidative stress. This can result in the oxidation of proteins, lipids, and DNA, and has been linked to the development and maintenance of several disease states, such as diabetes,[81] cardiovascular diseases,[82, 83] and Duchenne muscular dystrophy.[84, 85] One proposed mechanism for the link

between oxidative stress and disease is through modulation of apoptosis. Accumulating evidence suggests a role for the mitochondria in mediating oxidative stress by way of electron leak from the electron transport chain through incomplete reduction of molecular oxygen.[86, 87] This phenomenon can be induced in vitro in several ways, one of which is through direct addition of oxidant substances to cell culture media. A study examining the effects of mitochondria-targeted antioxidants used *t*-butylhydroperoxide, a powerful oxidant, to treat N_2A cells, resulting in a dose-dependent increase in intracellular ROS production and a concomitant decrease in cell viability.[88] Inhibition of certain elements of the electron transport chain also leads to electron leak and subsequent ROS production. In particular, myxothiazole and antimycin A (both mitochondrial complex III inhibitors) result in accumulation of electrons at complex III, promoting leak and formation of various ROS, such as H_2O_2 in heart, kidney, and skeletal muscle mitochondria.[89]

Two other significant sources of ROS include the xanthine oxidase and the NADPH oxidase enzyme systems. Xanthine oxidase (XO) is found in the cytosol of skeletal muscle, where it plays a major role in ROS production.[83, 90, 91, 92] It produces elevated levels of superoxide and hydrogen peroxide, as observed during ischemia-reperfusion injury of gastrocnemius muscles in rats.[83] Its activity has been shown to increase, along with markers of oxidative stress including protein carbonyls and lipid peroxides, in gastrocnemius muscles of rats exposed to a contraction-induced claudication exercise protocol.[91] On the other hand, NADPH oxidase produces superoxide anion that is rapidly dismutated to hydrogen peroxide, similar to the reactions mediated by xanthine oxidase. However, its cellular localization differs, in that NADPH oxidase is localized at the sarcolemma,[93] and in the t-tubules of skeletal muscle.[94] Skeletal muscle insulin resistance has recently been linked with angiotensin-II-

mediated ROS signalling involving NADPH oxidase, leading to activation of nuclear factor-κB.[95] There is also evidence that skeletal muscle sarcoplasmic reticulum contains a NADH oxidase that produces high levels of superoxide radical.[96]

With the abundant sources of oxidative stress outlined above comes the potential for damage both to intracellular structures and pro-survival factors. It has been demonstrated that apoptosome formation, a necessary step in caspase-9 activation and subsequent cell death, is intimately dependent upon ROS generation or leak of oxidants from the mitochondria.[97] Several studies have established a link between increasing levels of oxidative stress and subsequent elevations in apoptotic signalling. In particular, in vitro studies using the C2C12 mouse myoblast cell line have shown dose-dependent increases in DNA fragmentation, measured by TUNEL staining, a specific dye that stains for DNA strand breaks, and DNA laddering assessed by electrophoresis, upon treatment with hydrogen peroxide.[98] Recent evidence has shown that anti-apoptotic ARC protein levels are decreased via the ubiquitin-proteasome pathway in response to apoptotic stimuli such as oxidative stress.[99] Loss of mitochondrial membrane potential, accompanied by cytochrome c release and downregulation of ARC protein levels, have been observed in rat embryonic cardiac cells as a result of exposure to H_2O_2.[100] Similar releases of cytochrome c, as well as elevated DNA fragmentation, have been observed in murine macrophage cells exposed to increasing concentrations of 4-hydroxy-2,3-nonenal (4-HNE; an aldehydic by-product of lipid peroxidation).[101]

In further support of the link between oxidative stress and apoptosis, recent evidence indicates a role for antioxidants in preventing apoptosis in certain cell types and tissues. For instance, human satellite cells exposed to H_2O_2 show elevated TUNEL staining as well as increased protein carbonyl content, markers of apoptosis and oxidative stress, respectively.[50]

When these same cells were exposed to Oligopin, a natural antioxidant compound found in white pine bark, cell viability increased and all evidence of H_2O_2-induced apoptotic cell death was abolished.[50] Oxidative stress caused by inclusion of 4-HNE in growth media of Swiss 3T3 fibroblasts causes significant, dose-dependent DNA fragmentation and loss of cell viability; the antioxidant resveratrol has been shown to protect against these effects.[102] Additionally, studies employing knockout models of antioxidant enzymes show similar effects attributed to oxidative stress-mediated apoptosis. Mice heterozygous for *Sod*2 (or MnSOD), an important mitochondrial ROS scavenger, show increased sensitivity to mitochondrial permeability transition formation and subsequent release of cytochrome c upon challenge with calcium or *t*-butylhydroperoxide; the former is a commonly used source of ROS for in vitro experimentation.[103] Lens epithelium cells from *Sod*2 heterozygotic mice show dramatic mitochondrial damage, cytochrome c leak, caspase-3 activation and increased cell death compared to wild-type controls.[104] Transgenic mice that selectively overexpress human catalase, an important endogenous H_2O_2 detoxifier, in the mitochondria of skeletal and cardiac muscle display decreased H_2O_2 production from cardiac mitochondria compared to controls.[105] They also display increased lifespan, as well as decreased oxidative DNA damage throughout their lives, evidenced by decreased 8-hydroxydeoxyguanosine (8-OHdG) levels.[105] Similar protective effects of catalase overexpression have been observed in a murine cancer cell line, resulting in increased tumour growth.[106] There is also evidence for the deleterious effects of depletion of endogenous antioxidants, most notably reduced glutathione (GSH); however, this will be discussed in detail below. These studies highlight the link between apoptosis and redox status and suggest that conditions associated with increased oxidative stress may negatively influence apoptotic signalling.

Oxidative stress, aging and skeletal muscle apoptosis

It is proposed that a lifetime of electron flow through the mitochondria leads to cumulative damage by way of free radical production, particularly in post-mitotic tissues such as skeletal muscle;[87] this is known as the free radical or mitochondrial theory of aging. In the last several decades, scientists have begun to make a connection between normal aging and oxidative stress, especially with regards to skeletal muscle aging.[107, 108, 109, 110, 111] For example, aged animals display higher basal ROS production than their younger counterparts,[107] as well as higher protein carbonyl content and reduced expression of sulfhydryl groups in skeletal muscle mitochondria.[109] ROS have been shown to play an important role in age-associated mitochondrial dysfunction.[108, 111]

A common condition of aging in skeletal muscle is known as sarcopenia, involving significant loss of muscle mass and function, along with decreased basal metabolic rate.[112] In addition to this gradual loss of function, aging in skeletal muscle is also associated with selective loss of type II (fast-twitch) fibers, decreased muscle cross-sectional area, and general muscular dysfunction.[78] The mechanism of this selective loss of muscle fibers and associated muscle atrophy has been suggested to involve both oxidative stress and elevated levels of apoptosis.[56, 64, 72, 73, 76, 113] For instance, in aged humans displaying a high loss of type II muscle fibers, total superoxide dismutase (SOD) activity is significantly decreased, while markers of lipid peroxidation are increased.[76] In frail elderly humans, mRNA and protein levels of TNF-α, a main death-receptor ligand, are significantly elevated compared to younger adult controls.[113]

Animal studies using rodent models have shown comparable changes to humans. Specifically, muscles containing a higher proportion of type II fibers (ie. plantaris versus soleus) show elevated extrinsic pathway activation and specific fiber loss,[64] while older animals (24 months old) experience a 50% increase in mono- and oligonucleosomal DNA fragmentation compared to adult (6 month old) animals.[56] Additionally, caspase-3 is increased in aged EDL with no significant changes observed in soleus, providing further support for the selective loss of Type II fibers in aging.[73] TNF-α signalling is significantly elevated in old superficial vastus lateralis (predominantly type II muscle) compared to old soleus muscle.[72] Conversely, there is some evidence for increased apoptosis in type-I dominant soleus muscle of old animals, evaluated through increased apoptotic index and smaller cross-sectional area.[71] Furthermore, the more oxidative soleus muscle of rats shows a high basal level of pro-apoptotic Bax protein expression with a concomitant lower level of anti-apoptotic Bcl-2; the reverse trends are seen in the glycolytic, white gastrocnemius muscle, indicating a greater potential for apoptotic signalling in the more oxidative muscle type.[114] Yet others have shown elevated DNA fragmentation in both aged soleus and EDL muscles.[73] Taken together, these studies support the notion that apoptosis is elevated in skeletal muscle during aging. However, this evidence also indicates that the current consensus on selective fiber loss and aging-related muscle atrophy requires further clarification.

Glutathione: an important regulator of cellular redox status

Antioxidant enzymes and compounds are vital to maintenance of the delicate cellular redox balance. While many such compounds can be obtained from foods and supplements (exogenous antioxidants), the body has developed several endogenous defences against oxidative insult.[115, 116, 117] Specifically, the superoxide dismutases (CuZn- and Mn-containing)

are cellular enzymes that reduce the highly damaging superoxide anion ($O_2^{\cdot -}$) to hydrogen peroxide and molecular oxygen with the help of hydrogen.[117] Catalase is another important ROS detoxifier that exerts its action downstream of the superoxide dismutases by detoxifying H_2O_2 to water and molecular oxygen.[117] Another major intracellular antioxidant is reduced glutathione (GSH). It is expressed in all mammalian tissues, with levels varying from 0.2 mM to 10 mM depending on tissue type.[116] This water-soluble tripeptide is the major intracellular thiol composed of glutamate, glycine and cysteine and is synthesized in a two-step process. The first, rate-limiting, step consists of formation of the dipeptide γ-glutamylcysteine through ligation of L-cysteine and L-glutamate via the action of the enzyme γ-glutamylcysteine synthetase (γ-GCS, or Glutamate-L-Cysteine Ligase).[118] The second step is catalyzed by GSH synthetase, which adds a glycine residue to γ-glutamylcysteine, resulting in the fully functional tripeptide.[119]

Typically, glutathione is present in its reduced form (GSH) in the cell and may be oxidized to glutathione disulfide (GSSG) via detoxification of ROS by the glutathione peroxidase (GPx) enzyme system to which it contributes reducing equivalents.[120] It is rapidly reduced back to GSH by GSSG reductase (GR),[121] thus preserving the reducing cellular environment. There is a demonstrated relationship between vitamin C, an important water-soluble exogenous antioxidant, and GSH in their ability to "spare" each other through reduction reactions.[122] In particular, studies have shown that GSH is essential in maintaining the reduced form of vitamin C (ascorbate) in vivo, as depletion of GSH leads to oxidation of ascorbate to dehydroascorbate which is degraded and lost.[123] Similar mechanisms of mutual sparing have also been observed between vitamin E (an exogenous lipid-soluble antioxidant) and GSH, whereby each exerts its respective antioxidant activities to protect the other from

peroxide modification.[124] In addition, GSH can modulate the activity of a number of proteins through post-translational modification.[125] The ratio of GSH:GSSG is a useful indicator of cellular redox status and oxidative stress, with smaller values indicating an oxidative shift and larger values signifying a more reduced cellular state.[117]

Glutathione depletion by L-buthionine-[S,R]-sulfoximine

Attempts to evaluate the cellular redox status and the potential for cytoprotection by endogenous antioxidants due to various stressors has been attempted through GSH depletion both in cell culture and in animal models.[82, 126, 127, 128, 129, 130, 131, 132, 133, 134, 135, 136, 137, 138, 139] The vast body of literature on this biomolecule highlights its varied roles in many cellular functions. A large proportion of research literature has focused on chronic depletion of GSH to elucidate the degree of protection its presence confers upon cells. The most common depletion method uses specific inhibitors of elements of the γ-glutamyl cycle. A safe, established and effective method of obtaining this depleted model is use of the drug L-buthionine-[S,R]-sulfoximine (BSO), an inhibitor of γ-GCS.[140] Through inhibition of synthesis of GSH, levels are gradually depleted in almost all organ compartments in the body. BSO has been used to reliably deplete GSH in several tissues, including liver,[139, 140] kidney,[139, 140] pancreas,[139, 140] skeletal muscle,[139, 140] brain[139, 141] and heart.[82, 139]

Glutathione and apoptotic signalling

There is compelling evidence that intracellular glutathione is depleted acutely during apoptosis as part of death signal propagation, which may be effective in shifting the oxidative balance without necessarily causing overproduction of ROS.[129, 142] This local GSH depletion has been attributed to GSH extrusion from the cell during apoptosis[30, 126, 143, 144] or as a result of

cleavage of enzymes involved in GSH synthesis.[145] For instance, Jurkat cells, a T lymphocyte cell line, experience rapid intracellular depletion of GSH due to stimulation of extracellular death receptors by Fas/APO-1-activating antibody.[144] Apoptosis induced by a variety of agents in thymocytes leads to disruption of the mitochondrial membrane potential, production of ROS, and depletion of GSH in the early stages of apoptosis.[146] Further evidence for the relationship between cellular GSH levels and mitochondrial membrane potential fluctuations comes from studies using bongkrekic acid (BA), an inhibitor of the adenine nucleotide transporter (ANT) located on the inner mitochondrial membrane. ANT is one of the proposed channels involved in mitochondrial permeability transition (MPT), leading to release of pro-apoptotic factors into the cytosol.[38] BA has been shown to inhibit several apoptotic events associated with MPT, such as generation of ROS, DNA fragmentation, and local depletion of GSH.[147] Cells overexpressing anti-apoptotic Bcl-x_L are protected from GSH extrusion when exposed to an apoptotic challenge, but similar cells overexpressing pro-apoptotic Bax experience a significant loss of GSH prior to apoptosis onset, highlighting the cooperation between GSH and Bcl-x_L in promoting cell survival.[126] Activation of plasma membrane GSH transporters in hepatic cells can be increased by treatment with extrinsic pathway death ligands,[143] while Bcl-2 overexpression in HeLa cells helps to conserve intracellular GSH levels by inhibiting a methionine-dependent efflux pump.[148] Bcl-2 overexpression in other cell lines, such as the GT1-7 hypothalamic line, has shown similar anti-apoptotic effects when glutathione depletion is induced. In fact, basal GSH levels have been reported up to 3 orders of magnitude higher in Bcl-2 overexpressors compared to controls, an effect that is conserved even when BSO is used to deplete intracellular GSH stores.[149] Exposure of apoptosis-resistant lymphoma cells to cysteine/methionine-free culture media restores apoptotic sensitivity,

comparable to the irradiation-sensitive lymphoma cell line; this effect is mediated by a drop in intracellular GSH levels.[150] Lastly, Bcl-2 overexpression has been shown to cause localization of GSH to the nucleus, leading to prevention of caspase activation and subsequent apoptotic death.[151] In addition to the above links between apoptotic signalling and GSH, caspase-3 has been shown to mediate cleavage of the catalytic subunit of γ-GCS, resulting in depletion of GSH due to loss of enzyme activity and de novo GSH synthesis.[145]

Use of the BSO-induced glutathione depletion model has shed light on the interaction between intracellular GSH levels and risk of apoptotic events. For instance, apoptotic signalling is associated with increased ROS production due to glutathione depletion by BSO in a B cell lymphoma line.[152] Mitochondrial permeability transition was shown to be activated in BSO-treated HL-60 cells, a human leukemia cell line; this effect was mediated by mitochondrial ROS generation.[153] Chronic glutathione depletion through an engineered cell line has been shown to increase apoptotic markers in as little as 48 hours.[154] In addition, severe mitochondrial damage has been attributed to BSO-induced GSH depletion. In mitochondria isolated from the brains of newborn rats, GSH depletion leads to mitochondrial swelling and degeneration.[141] BSO has also been shown to be effective in inducing estrogen-mediated apoptosis in a human breast cancer cell line characterized by its high intracellular GSH stores.[155]

Alternatively, increasing GSH levels as a protective mechanism against apoptosis has shown some success. For example, GSH has been shown to prolong survival in cancer cell lines.[128] Mice fed a sulphur amino-acid enriched diet (supplemented with 1% L-cysteine and 1% GSH) experienced a 63% increase in hepatic GSH levels.[52] These animals were subsequently injected with an antagonistic anti-Fas antibody and showed preserved

GSSG:GSH ratio, prevention of mitochondrial permeabilization and hepatic apoptosis compared to age-matched controls fed a normal chow diet.[52] Activated human T cells display an apoptosis-resistant phenotype upon exposure to Fas when supplemented with glutathione monoesters or N-acetylcysteine (NAC; a thiol antioxidant and precursor to GSH). This effect was completely abolished when cells were subjected to BSO-induced GSH depletion.[156] Collectively, this data demonstrate the potentially protective relationship between intracellular GSH levels and apoptotic signalling, wherein maintenance of thiol levels results in an anti-apoptotic phenotype.

Purpose

There are established links between oxidative stress and apoptosis, along with the consistent observation of increased oxidative stress as a result of both aging and glutathione depletion by BSO. Studies on the effect of GSH depletion on apoptosis have been carried out in a variety of tissues; however, little is known about these effects in skeletal muscle. Therefore, the purpose of the present study was to examine the role of glutathione in skeletal muscle apoptotic signalling, with particular emphasis on muscles composed of different fiber types. Antioxidant redox status changes, as well as shifts in antioxidant capacity were examined in soleus, a predominantly slow-twitch, oxidative muscle, and contrasted to the white portion of the gastrocnemius, a predominantly fast-twitch glycolytic muscle. Apoptotic protein expression and DNA fragmentation were also determined in these two muscle types. In addition, the effects of aging on skeletal muscle apoptosis, in combination with the oxidative challenge of glutathione depletion, were evaluated.

Objectives

The primary aim of the present study is to investigate the role of GSH depletion in apoptotic signalling in skeletal muscle. Given the unclear relationship between apoptotic signalling and GSH in skeletal muscle, a GSH depletion model will be used to better understand the importance of antioxidant status in apoptotic signalling in this tissue. Soleus and white portions of the gastrocnemius muscle have been chosen for analysis due to their established differences in oxidative potential and relatively pure fiber type composition (Soleus predominantly type I, WG predominantly type IIB). A secondary aim of this study is to elucidate the effect of advancing age on apoptotic signalling in GSH-depleted and GSH-intact skeletal muscle. There is an established link between apoptotic signalling and aging; however, the effect of GSH depletion on apoptosis in skeletal muscle of older animals is currently unclear.

Hypotheses

The hypotheses of the current work are as follows:

1. BSO treatment will decrease muscle GSH and increase muscle ROS production in both slow and fast skeletal muscle types. This effect will be further amplified in older animals.

2. Skeletal muscle from older animals will experience higher levels of oxidative stress compared to their younger counterparts; this will be independent of BSO treatment status.

3. In addition, upregulation of antioxidant enzymes will be observed primarily in the older animal groups, with the highest values seen in the old BSO-treated group.

4. The hypothesized increases in oxidative stress will lead to increased markers of apoptotic signaling in both soleus (slow) and white gastrocnemius (fast) muscle, with the highest increases observed in older, BSO-treated animals.

5. Levels of apoptotic markers will be increased in SOL compared to WG, as there are established differences in basal apoptotic expression in these muscle types. This will be independent of BSO treatment status.

METHODS

Animals

Male Sprague-Dawley rats were obtained from an in-house breeding colony (University of Waterloo, Waterloo, ON) for inclusion in this study. Two age groups were examined: a "young" group made up of adult-aged animals (34.85 ± 0.14 weeks; n=24) and an "old" group consisting of approximately middle-aged animals (69.11 ± 0.74 weeks; n=24). Rats were housed in a controlled environment at constant air temperature (20-21˚C) and humidity (~50%) on a 12h:12h reversed light/dark cycle. Standard Teklad 22/5 rodent chow (Harlan, WI) was provided, with intake monitored daily. All animal care procedures were approved by the University of Waterloo Animal Care Committee.

BSO treatment

The drug L-buthionine-[S,R]-sulfoximine (BSO; BioShop Canada Inc.), a specific γ-glutamylcysteine synthetase inhibitor, was used to deplete glutathione levels. The young and old rats were subdivided into control (CON) and BSO-treated (BSO) groups, resulting in four experimental groups: Young CON (n=12), Young BSO (n=12), Old CON (n=11) and Old BSO (n=13). Control animals were provided regular drinking water while BSO-treated animals were given water containing 30mM BSO ad libitum for 10 consecutive days, with intake recorded daily. Water was changed every 2 days, due to the limited half-life of the BSO drug. Body weight of all animals was determined prior to BSO administration as well as after the 10 day treatment period in order to assess possible drug toxicity.

Tissue collection

At the end of the 10 day drug treatment, the BSO-treated rats and age-matched controls were anesthetized with sodium pentobarbital (90-100mg/kg body weight) and sacrificed by removal of the heart. Soleus and white portions of the gastrocnemius muscle were quickly isolated. The majority of excised muscle was quickly snap frozen in liquid nitrogen and stored at -80˚C for further biochemical analyses. A small portion of the muscle belly of each muscle type was covered in Tissue-Tek Optimal Cutting Temperature medium (Sakura Finetek, USA), quickly frozen in liquid nitrogen-cooled isopentane, and stored at -80˚C for immunohistochemical analyses.

Immunoblot analyses and subcellular fractionation

For whole muscle homogenates, skeletal muscle (~20-25mg) was homogenized in 19 volumes of ice-cold muscle lysis buffer (20mM HEPES, 10mM NaCl, 1.5mM $MgCl_2$, 1mM DTT, 20% glycerol and 0.1% Triton X100; pH 7.4) with protease inhibitors (Complete Cocktail; Roche Diagnostics) using a glass homogenizer. Homogenates were then centrifuged at 1000 x *g* for 10 minutes at 4˚C, the supernatant was collected, and total protein was determined by the BCA protein assay.

Subcellular fractions of muscle were prepared by differential centrifugation (see Figure 3). Briefly, skeletal muscle (45mg for soleus, 60-65mg for white gastrocnemius) was homogenized by hand in 19 volumes of ice-cold mitochondrial isolation buffer (250mM sucrose, 20mM HEPES, 10mM KCl, 1mM EDTA, 1mM EGTA, 1mM DTT; pH 7.4) with protease inhibitors (Complete Cocktail; Roche Diagnostics) using a glass homogenizer. Homogenates were centrifuged at 800 x *g* at 4°C for 10 minutes, yielding a pellet (P1) and

supernatant (S1). The resulting S1 fraction was spun at 800 x *g* at 4°C for an additional 10 minutes to remove any residual debris and the resulting supernatant transferred to a new tube (S2). The S2 fraction was then spun at 20,800 x *g* at 4°C for 20 minutes to yield a pellet containing the mitochondrial fraction (M1) and a supernatant corresponding to the cytosolic fraction (C1). The M1 pellet was washed twice by adding mitochondrial isolation buffer and centrifuged at 20,800 x *g* at 4°C for 20 minutes. The resulting pellet was considered the enriched mitochondrial fraction. The C1 supernatant was re-spun two additional times at 20,800 x *g* at 4°C for 20 minutes to remove any residual mitochondria and debris, resulting in a cytosolic-enriched fraction. The P1 pellet obtained from the first spin of the whole muscle homogenate was washed with mitochondrial isolation buffer and spun at 800 x *g* at 4°C for 10 minutes three additional times. The remaining pellet at this stage was combined with 200 µL of muscle lysis buffer and 27.7 µL of 5M NaCl, and rotated for 1 hour at 4°C. The samples were then centrifuged at 20,800 x *g* at 4°C for 15 minutes, with the resultant supernatant kept as the nuclear-enriched fraction. Total protein concentration was determined for each fraction by the BCA protein assay and immunoblots performed to verify the purity of fractions using the following primary antibodies: rabbit polyclonal anti-histone H2B (Cell Signaling Technology) for the nuclear fraction, rabbit polyclonal anti-copper zinc superoxide dismutase (CuZnSOD) (Stressgen Bioreagents) for the cytosolic fraction, and goat polyclonal anti-adenine nucleotide translocase (ANT) (Santa Cruz Biotechnology) for the mitochondrial fraction. Samples were then stored at -80°C for further immunoblot analysis.

Equal amounts of protein were loaded in duplicate and electrophoresed on 12% or 15% SDS-PAGE gels, transferred onto PVDF membrane (Bio-Rad Laboratories), and blocked overnight with 5% milk in Tris-Buffered Saline with 0.1% Tween (TBS-T) at 4˚C. Membranes

with whole homogenate samples were incubated at room temperature for 1 hour with the following primary antibodies: mouse monoclonal anti-apoptosis inducing factor (AIF), rabbit polyclonal anti-apoptosis repressor with caspase recruitment domain (ARC), rabbit polyclonal anti-Bax (Santa Cruz Biotechnology); rabbit polyclonal anti-CuZnSOD, mouse monoclonal anti-heat shock protein 70 (Hsp70), rabbit polyclonal anti-manganese superoxide dismutase (MnSOD), rabbit polyclonal anti-second mitochondrial activator of caspases (Smac) (Stressgen Bioreagents); and rabbit polyclonal anti-catalase (Sigma-Aldrich). For detection of Bcl-2 and 4HNE in whole homogenates, membranes were blocked with 5% TBS-T at room temperature for 1 hour then incubated with either a mouse monoclonal anti-Bcl-2 primary antibody (Santa Cruz Biotechnology) or a rabbit polyclonal anti-4HNE primary antibody (Abcam) for 1-2 hours at room temperature, followed by further incubation at 4ºC overnight. The subcellular fractions obtained were also electrophoresed and blocked as specified above, with different proteins examined in the various fractions. AIF detection was performed in both the nuclear and cytosolic fractions in both tissues, and in mitochondrial fractions of WG only (due to limited sample), while Smac and cytochrome c (mouse monoclonal primary; Santa Cruz Biotechnology) were examined in the cytosolic fraction of SOL and WG as an indirect marker of mitochondrial release of these proteins. Membranes were then washed with TBS-T and incubated with the appropriate species-specific horseradish peroxidase (HRP)-conjugated secondary antibody (Santa Cruz Biotechnology) for 1 hour at room temperature, washed, and visualized using the Amersham Enhanced Chemiluminescence Western Blotting detection reagents (GE Healthcare) and the ChemiGenius 2 Bio-Imaging System (Syngene). The only deviations from these steps was in the detection of Bcl-2, whereby 2 hours of secondary antibody incubation was used in combination with the Amersham ECL Plus detection reagents

(GE Healthcare). The approximate molecular weight for each protein of interest was estimated using Precision Plus Protein WesternC Standards in conjunction with Precision Protein Streptactin HRP Conjugate (BioRad Laboratories). Equal loading and quality of protein transfer was evaluated by Ponceau S staining (Sigma-Aldrich). Protein levels are expressed as mean relative optical density in arbitrary units (AU).

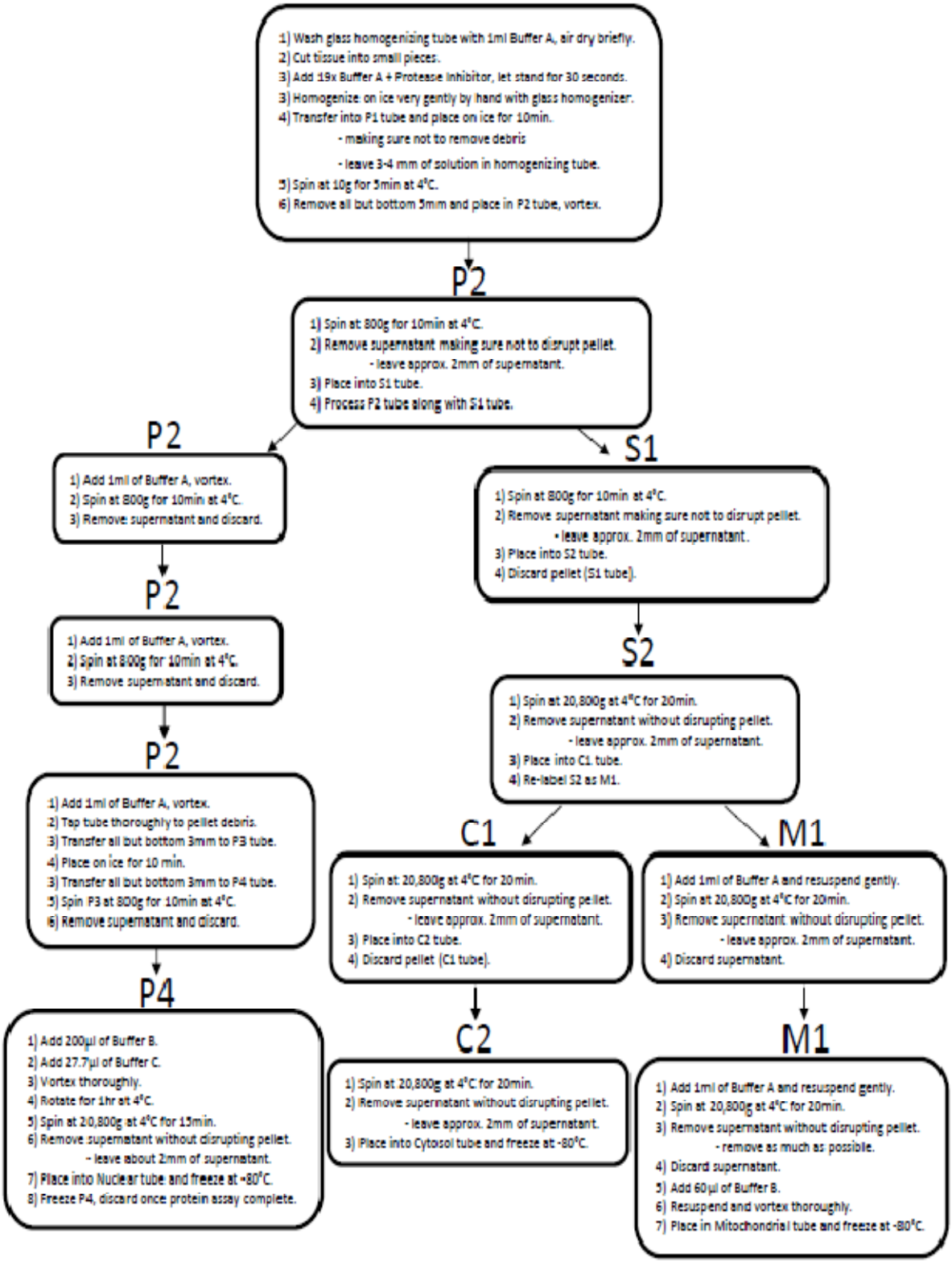

Figure 3: Differential centrifugation protocol (Quadrilatero Lab)

Glutathione quantification

Reduced glutathione (GSH) and oxidized glutathione (GSSG) levels were determined by high-performance liquid chromatography (HPLC).[157] Briefly, 20-25 mg of muscle tissue was homogenized on ice in 10 volumes of 2mM phenanthroline in 7% perchloric acid using a glass homogenizer. After a brief incubation on ice, samples were centrifuged at 1000 x *g* for 10 minutes at 4˚C. A portion of the supernatant (125µL) was removed, treated with 5µL of 0.4 M iodoacetic acid, and neutralized with excess $NaHCO_2$. Samples were then incubated in the dark at room temperature for 1 hour, after which time they were treated with 1µL 1-fluoro-2,4-dinitrobenzene (1.5mL in 98.5mL absolute ethanol), and further incubated in the dark for 8 hours. A 25µL aliquot of each sample was run on a Waters Alliance 2695 system using a Varian (Rainin) Microsorb 5µM amino (25cm x 4.5cm) column at room temperature for 35 minutes with a flow rate of 1mL/min, and detected at 350 nm.

Reactive Oxygen Species generation

Reactive oxygen species (ROS) generation was determined using 2',7'dichlorohydrofluorescein-diacetate (DCFH-DA) as previously performed.[9, 107] DCFH-DA is hydrolyzed by intracellular esterases to yield nonfluorescent DCFH, which is oxidized to the highly fluorescent compound DCF as a result of ROS exposure. Briefly, ~10 mg of muscle tissue was homogenized in ice-cold Phosphate-Buffered Saline (PBS; pH 7.4) using a glass homogenizer. Duplicates of whole muscle homogenate were pre-incubated with the ROS scavenger Tiron (1mM) as a negative control, or left untreated. Samples were then incubated in the dark with 5µM DCFH-DA (Invitrogen) at 37˚C. Fluorescence was measured every 15 minutes for 2 hours using a SPECTRAmax GEMINI XS microplate spectrofluorometer

(Molecular Devices) with excitation and emission wavelengths of 490 nm and 525 nm, respectively. Fluorescence intensity was normalized to total protein content and expressed as AU per mg protein.

Caspase proteolytic enzyme activity

The enzyme activity for caspase-3, caspase-8, and caspase-9 was determined spectrofluorimetrically in muscle homogenate using the fluorescent substrates Ac-DEVD-AMC, Ac-IETD-AMC, and Ac-LEHD-AMC (Enzo Life Sciences), respectively. Briefly, 12-15mg of tissue was homogenized in ice-cold muscle lysis buffer, without protease inhibitors, and centrifuged at 1000 x *g* for 10 minutes at 4˚C. Tissue supernatants were then incubated with the appropriate substrate at room temperature for 2 hours. Fluorescence was measured every 15 minutes using a SPECTRAmax Gemini XS microplate spectrofluorometer (Molecular Devices) with excitation and emission wavelengths of 360 nm and 440 nm, respectively. In control experiments, caspase substrates were incubated with either human recombinant active caspase-3 (Enzo Life Sciences), caspase-8 (Sigma-Aldrich), or caspase-9 (Enzo Life Sciences). In all cases, a strong fluorescent signal was obtained, indicating the specificity of the selected substrates. In addition, incubation of active recombinant enzymes as well as muscle samples with inhibitors for caspase-3 (Ac-DEVD-CHO; Enzo Life Sciences), caspase-8 (Ac-IETD-CHO; Sigma-Aldrich), and caspase-9 (Ac-LEHD-CHO; Enzo Life Sciences) completely inhibited the fluorescent signal observed. Caspase activity was normalized to total protein content and expressed as AU per mg protein.

DNA fragmentation assay

Cytoplasmic histone-associated mono- and oligonucleosomes (ie. from fragmented DNA) were determined using the Cell Death Detection ELISA^{PLUS} Kit (Roche Diagnostics) according to the manufacturer's instructions. Briefly, 5-7 mg of muscle tissue was homogenized in the lysis buffer provided, incubated for 30 minutes at room temperature and centrifuged at 200 x *g* for 10 minutes at room temperature. A 20 µL aliquot of supernatant was incubated with 80 µL of anti-histone-biotin/anti-DNA-peroxidase reagent in a streptavidin-coated microplate for 2 hours at room temperature with gentle shaking (~300 rpm). The solution was then aspirated from each well, washed 3 times with the incubation buffer provided in the kit, replaced with 100 µL of 2,2'-azino-bis(3-ethylbenzthiazoline-6-sulphonic acid) (ABTS) substrate solution and incubated for a further 30 minutes at room temperature. Absorbance measurements were taken every 5 minutes using a SPECTRAmax Plus spectrophotometer (Molecular Devices) at 405 nm and 490 nm. A control sample consisting of a DNA-histone complex was included to confirm a positive signal for DNA fragmentation. Absorbance was normalized to total protein content and expressed as AU per mg protein.

Immunohistochemical analyses

Lipid peroxidation due to oxidative stress

Skeletal muscle cross-sections (10 µm) were obtained using a Shandon Cryotome SME (Thermo Electron Corp.). Muscle cross-sections were examined for lipid peroxidation using immunofluorescence staining for 4-hydroxynonenal (4-HNE) content. 4-HNE is the primary α,β-unsaturated hydroxyalkenal produced in cells as a result of oxidative insult;[95] in particular, expression of this peroxidation product has been observed in skeletal muscle exposed to

oxidative stress[158]. Frozen slides were thawed, air dried and fixed in 4% paraformaldehyde. Next, slides were blocked in 5% goat serum for 30 minutes, and then incubated for 1 hour in a humidified chamber with the same rabbit polyclonal anti-4-HNE primary antibody (AbCam) used for immunoblot analysis. Sections were washed in PBS and then incubated in the dark in a humidified chamber with a goat anti-rabbit IgG-FITC secondary antibody (Santa Cruz Biotechnology) for 1 hour, washed in PBS, and mounted in ProLong Gold Antifade Reagent (Invitrogen). Sections were visualized using a Zeiss Axio Observer Z1 structured-illumination fluorescent microscope equipped with an AxioCam HRm camera and associated AxioVision 4.7 imaging software (Carl Zeiss).

ARC staining

Muscle cross-sections were thawed and air dried, then fixed in 100% acetone at 4°C for 10 minutes and air dried for an additional 5 minutes. They were washed in PBS and subsequently permeabilized in 0.5% Triton X-100 for 5 minutes. After washing, 0.6% hydrogen peroxide (H_2O_2) was applied to sections for 10 minutes to quench endogenous peroxidase activity. Sections were then washed and blocked with 5% goat serum in PBS for 30 minutes in a humidified chamber, and subsequently incubated for 1 hour with the same rabbit polyclonal anti-ARC antibody (Santa Cruz Biotechnology) used for immunoblot analysis. Sections were then washed and incubated with an anti-rabbit IgG biotinylated secondary antibody (Vector Laboratories) for 1 hour, washed, and incubated with ABC Reagent for 30 minutes (Vector Laboratories). After another wash, the NovaRED peroxidase substrate kit (Vector Laboratories) was used, which produces a red precipitate at the target staining areas; the stain was left on the slides for 13-15 minutes. Slides were rinsed with dH_2O to remove residual stain and washed once more in PBS before being mounted in glycerol gel medium and visualized

using a Nikon Eclipse 50i light microscope with a PixelLink Camera and associated imaging software.

Data analysis

Data is represented as means ± standard error of the mean for each experimental group. Group comparisons were conducted using a 2 X 2 ANOVA followed by Tukey post hoc analysis where appropriate. For comparison of approximate drug intake between young and old BSO-treated animals, a Student's t-test was performed. Except where otherwise indicated, data were normalized to the Young CON group for the muscle of interest. Statistical significance was set at $p<0.05$.

RESULTS

Anthropometric, water and food intake data

Anthropometric data, along with food and water intake for all experimental animals, can be found in Table 1. As expected, there was a significant difference in age ($p<0.01$) between the "young" and "old" groups (34.85 ± 0.14 versus 69.11 ± 0.74 weeks). Though there was no statistically significant effect for age in terms of water intake, the young groups consumed 10% more water than their older counterparts, on average. The interaction term for water intake was significant ($p<0.01$), indicating that the Young BSO animals consumed up to 34% more water than the Old BSO group during the 10-day treatment period. A significant age-related decrease in approximate BSO dose was seen, from $3.74x10^{-3} \pm 0.24x10^{-3}$ mmol/g/day in Young BSO to $2.33x10^{-3} \pm 0.14x10^{-3}$ mmol/g/day in Old BSO. The Old BSO group also consumed significantly less food than all other groups, as assessed by the interaction term ($p<0.05$) for this measure. Additionally, BSO dose was inversely correlated with post-treatment body weight ($r=-0.789$, $p<0.001$) as well as kidney weight ($r=-0.743$, $p<0.001$), whereby higher BSO doses corresponded to lower body and kidney weights. There was also a significant ($p<0.01$) age-related increase in kidney weight compared to younger animals.

Prior to BSO treatment, a significant ($p<0.01$) main effect for age was observed in pre-treatment body weight, whereby old animals weighed more than their younger counterparts. A similar age-related effect persisted after treatment; in addition, BSO-treated animals experienced significant ($p<0.01$) decreases in body weight compared to age-matched controls as assessed by the average change in weight from pre- to post-treatment. A main effect for age ($p<0.01$) was also observed for this measure, whereby older animals lost significantly more weight than younger animals over the course of the treatment period. Lastly, muscle cross-

sectional area, used to assess possible losses of muscle mass in place of the muscle wet weight, showed a main effect ($p<0.05$) for age in SOL, with 15% higher values observed in old compared to young animals. WG tissue also displayed a significant main effect ($p<0.05$) for age, but older animals had 16% lower muscle cross-sectional area than their younger counterparts.

Table 1: Anthropometric, water and food intake for all experimental animals

	Young CON (YCON, n=12)	Young BSO (YBSO, n=12)	Old CON (OCON, n=11)	Old BSO (OBSO, n=13)	P_{BSO}	P_{AGE}	$P_{BSOxAGE}$
Age (wks)	35.11 ± 0.23	34.60 ± 0.13	69.73 ± 1.11	68.58 ± 1.00	NS	<0.001	NS
Water intake (mL)	482.3 ± 19.12	604.75 ± 30.12	544.91 ± 49.09	452.23 ± 29.56	NS	NS	0.002
Total food intake (g)	233.36 ± 6.88	207.77 ± 6.16	230.66 ± 9.46	170.72 ± 10.44	<0.001	0.037	0.036
Approx. BSO dose (mmol/g/day)	0	$3.74x10^{-3}$ $\pm0.24x10^{-3}$	0	$2.33x10^{-3}$ $\pm0.14x10^{-3}$	---	<0.001	---
Pre-BSO body weight (g)	506.15 ± 7.92	494.29 ± 6.39	585.48 ± 14.95	611.94 ± 14.73	NS	<0.001	NS
Post-BSO body weight (g)	510.27 ± 7.85	480.07 ± 5.84	575.39 ± 14.03	554.28 ± 9.75	0.012	<0.001	NS
Average weight change (g)	4.13 ± 1.79	-14.22 ± 2.78	-10.09 ± 2.87	-57.66 ± 15.24	0.001	0.002	NS
Kidney weight (g)	1.43 ± 0.04	1.39 ± 0.03	1.84 ± 0.04	1.90 ± 0.04	NS	<0.001	NS
SOL Muscle CSA (μm^2)*	5562.52± 221.02	5644.18± 149.56	6688.08± 512.33	6154.20 ± 292.12	NS	0.017	NS
WG Muscle CSA (μm^2)*	5469.10± 397.20	4895.41± 449.44	4283.74± 264.97	4434.16± 321.52	NS	0.04	NS

*for cross sectional area (CSA) data, n=8 was used

BSO treatment alters glutathione content

Reduced glutathione (GSH) content, as measured by HPLC, showed a significant ($p<0.05$) main effect for drug treatment, as GSH was significantly decreased in SOL and WG tissues compared to age-matched controls. SOL GSH decreased 89% from controls to BSO-treated animals (Figure 4), while in WG GSH similarly decreased 96% (Figure 5). Glutathione disulfide (GSSG) content followed a similar pattern to that observed for GSH. Namely, GSSG levels were not affected by age in either tissue but were decreased 89% ($p<0.001$) in WG due to BSO treatment compared to controls (Figure 5). There was a significant interaction ($p<0.05$) effect in SOL GSSG, whereby both BSO groups were decreased compared to the Young CON group. Additionally, the Young CON group was decreased compared to the Old CON's (Figure 4).

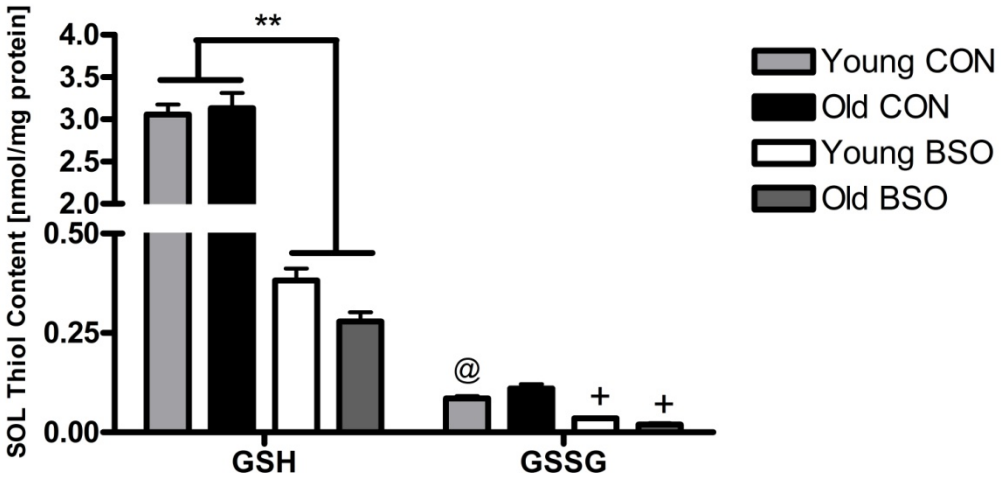

Figure 4: GSH and GSSG levels in soleus (SOL) muscle; values are presented as means ± SEM.
** indicates main effect for BSO ($p<0.001$); @ significantly different than Old CON ($p<0.05$); + significantly different than Young CON and Old CON ($p<0.001$).

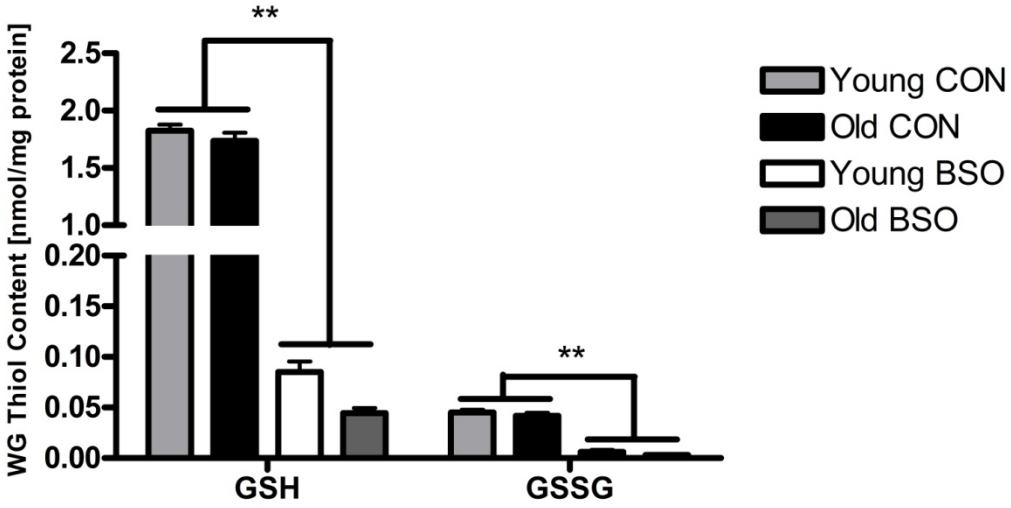

Figure 5: GSH and GSSG levels in white gastrocnemius (WG) muscle; values are presented as means ± SEM. ** indicates main effect for BSO ($p<0.001$).

BSO treatment also significantly impacted the GSH:GSSG ratio, a commonly-used indicator of cellular redox status. BSO-treated groups were significantly ($p<0.05$) decreased by 62% in the WG tissue compared to age matched controls. A significant interaction ($p<0.05$) was observed in the SOL, whereby both the Young BSO and Old BSO groups were significantly reduced compared to the controls, respectively (Figure 6).

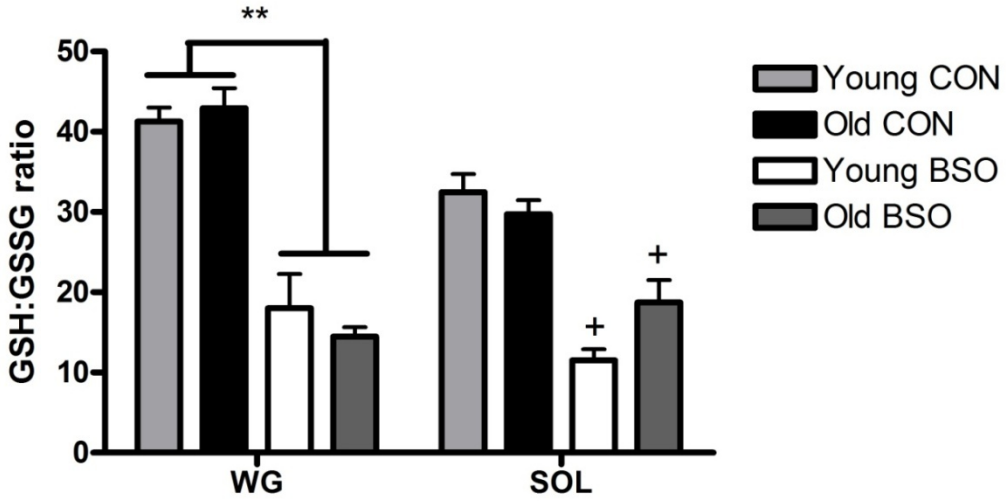

Figure 6: GSH:GSSG ratios in WG and SOL tissues; values are presented as means ±SEM. ** indicates main effect for BSO ($p<0.001$); + significantly different than Young CON and Old CON ($p<0.05$).

BSO treatment leads to increased ROS production only in SOL in the absence of similar effects on lipid peroxidation

ROS production was determined in muscle homogenate by measuring DCFH oxidation. BSO treatment led to significantly ($p<0.05$) increased ROS production in SOL muscles compared to age-matched controls (Figure 7). ROS production was not different between groups in WG muscle (Figure 7).

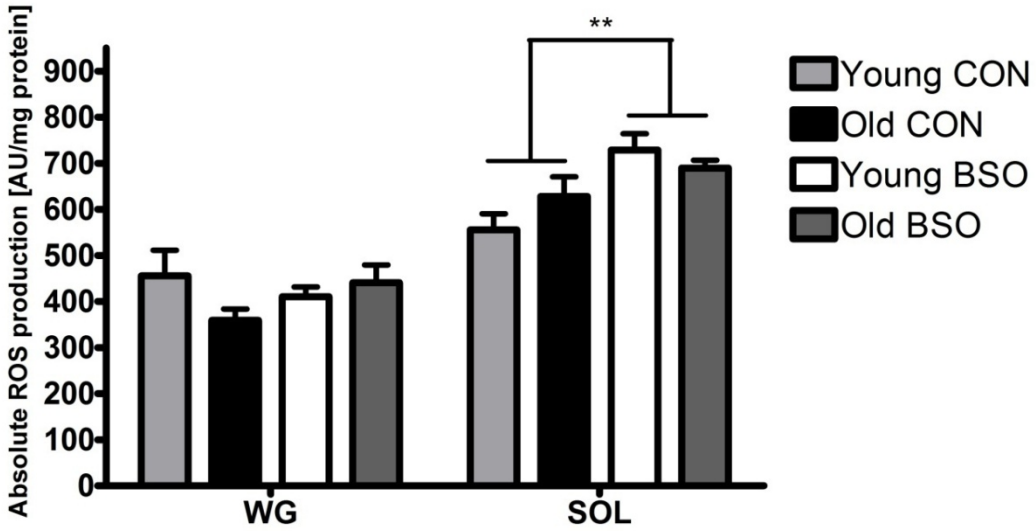

Figure 7: ROS production in SOL and WG muscle; all values are represented as arbitrary fluorescent units per mg protein. ** indicates main effect of BSO ($p<0.05$).

In contrast to the observed increase in ROS production, 4 hydroxy-2-nonenal (4HNE) levels were not significantly different between groups in both WG and SOL as measured by immunoblot analysis (Figure 8). There was a nonsignificant trend ($p=0.097$) toward a 37% decrease in 4HNE protein levels in BSO animals compared to controls in SOL. Immunofluorescence analysis did, however, show a 15% decrease ($p<0.05$) in 4HNE staining in BSO-treated SOL tissue compared to age-matched controls (Figure 9, panels B and C). While this is contrary to the hypothesized increase in oxidative stress in this model, part of this

observed effect may be due to the substantial amount of variability within each tissue. There was a pronounced difference in staining pattern between SOL and WG tissues, with higher staining intensity observed around the plasma membrane in the more oxidative SOL tissue and whole-section staining in the WG. The extremely high fluorescence observed on the periphery of muscle fibers contributed to the significant ($p<0.05$) main effect seen between tissues, with SOL muscle displaying slightly higher overall fluorescence than WG (Figure 9, all panels).

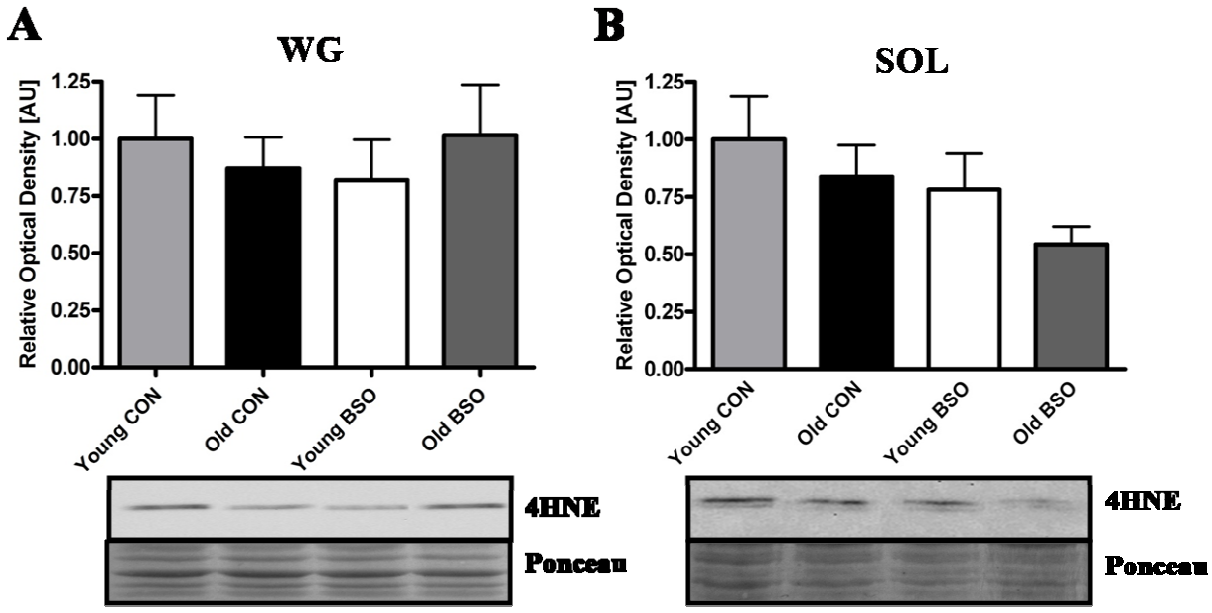

Figure 8: 4HNE quantification by immunoblot densitometry. Panel A shows representative immunoblots, ponceau images and densitometric analysis for WG, while Panel B shows representative immunoblots, ponceau images and densitometric analysis for SOL. All values are relative optical densities normalized to respective Young CON and expressed as means ± SEM.

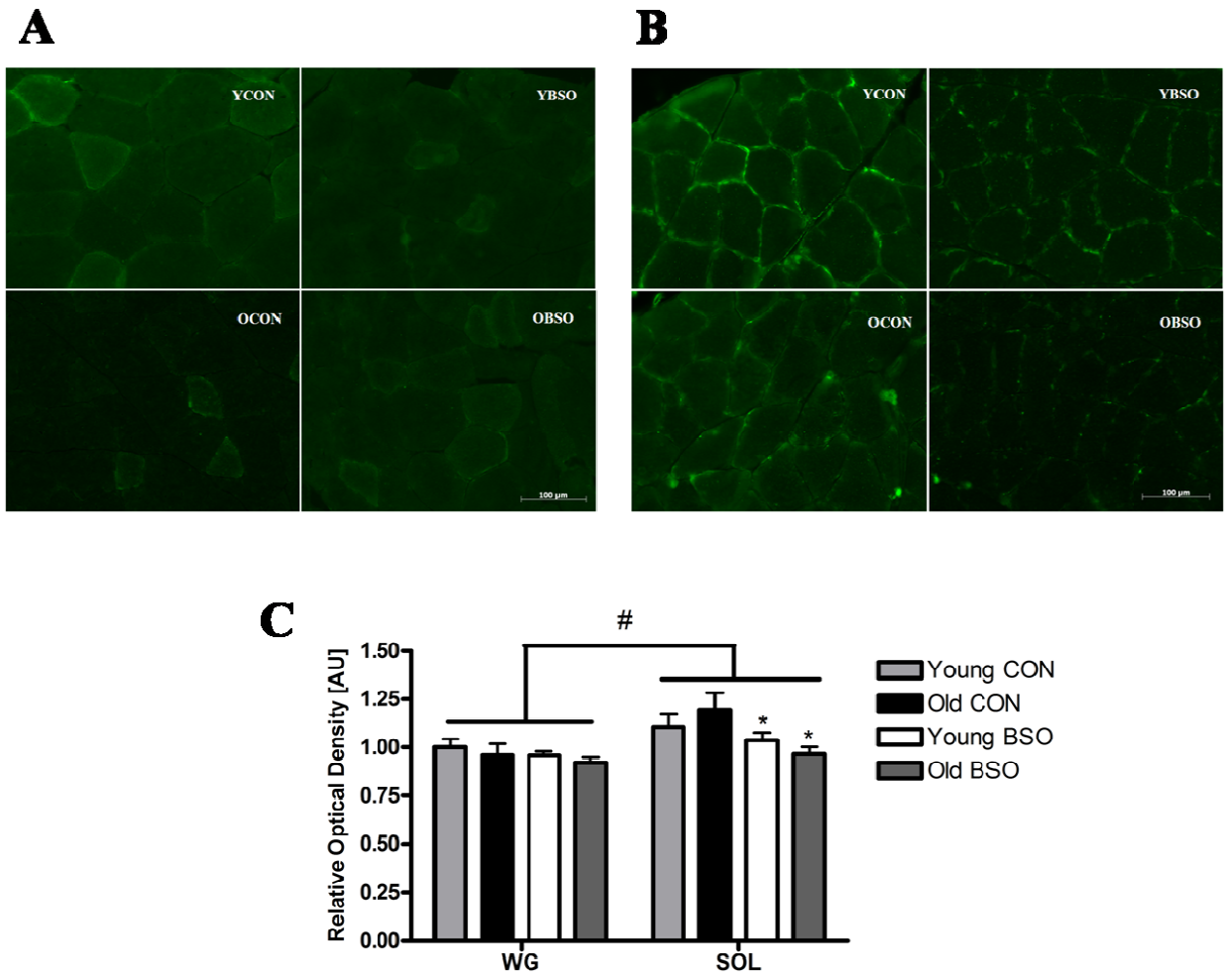

Figure 9: Results of 4HNE immunofluorescent staining and quantitative analysis of muscle cross sections from all experimental groups. Panel A shows the representative photomicrographs of WG 4HNE staining; Panel B shows the representative photomicrographs of SOL 4HNE staining. Scale bar is 100µm. YCON: Young CON; YBSO: Young BSO; OCON: Old CON; OBSO: Old BSO. Panel C shows quantitative analysis of immunofluorescent staining. Values are normalized to WG Young CON and expressed as means ± SEM. *indicates a main effect for BSO treatment ($p<0.05$); #indicates a main effect for tissue ($p<0.05$).

Glutathione depletion leads to increased catalase expression in SOL and WG

The protein expression of several antioxidant enzymes was examined by immunoblot analysis. There were no significant differences observed in CuZnSOD or MnSOD protein expression in either SOL (Figure 10) or WG (Figure 11). In contrast, there was a significant ($p<0.001$) 1.5-fold increase in catalase expression due to both age and BSO treatment in SOL tissue (Figure 10). In WG tissue, the significant interaction term ($p<0.05$) indicated higher catalase

expression in the Old BSO group compared to all other groups. In addition, catalase expression was higher in the Young BSO and Old BSO groups compared to Young CON (Figure 11). Overall, a 1.5-fold increase in catalase was seen due to age and a 1.7-fold increase in BSO-treated animals compared to age-matched controls in WG.

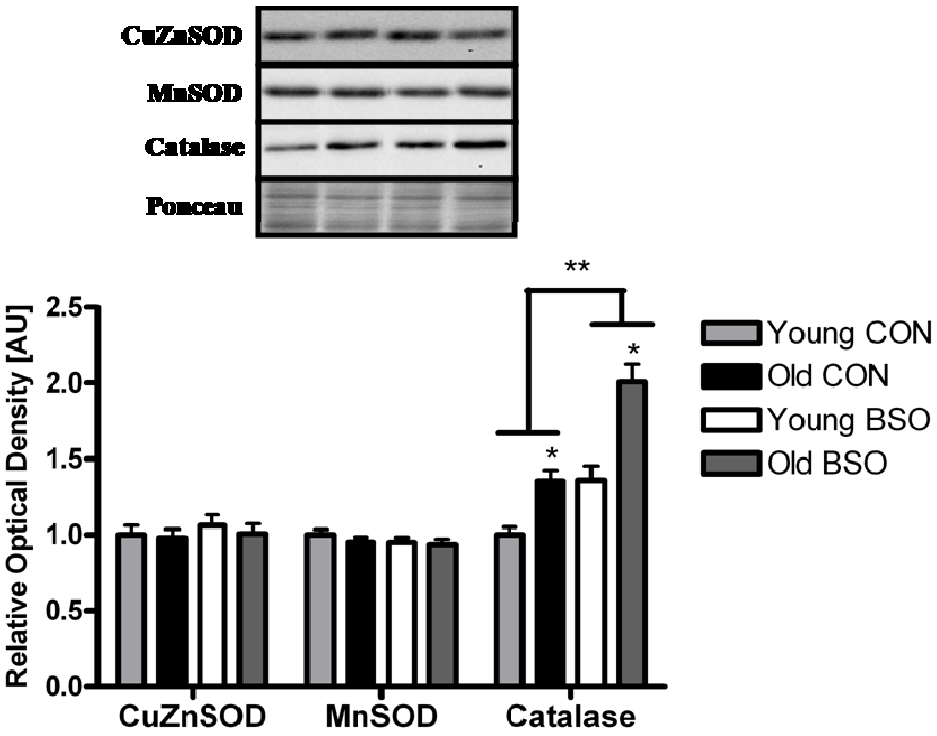

Figure 10: SOL antioxidant protein levels across all 4 experimental groups as assessed by densitometry. Representative immunoblots are shown, with a ponceau image to show equal protein loading; from left to right, lane 1: Young CON, lane 2: Old CON, lane 3: Young BSO, lane 4: Old BSO. All values are relative optical densities normalized to Young CON and expressed as means ± SEM. * indicates main effect for AGE ($p<0.001$); ** indicates main effect for BSO treatment ($p<0.001$).

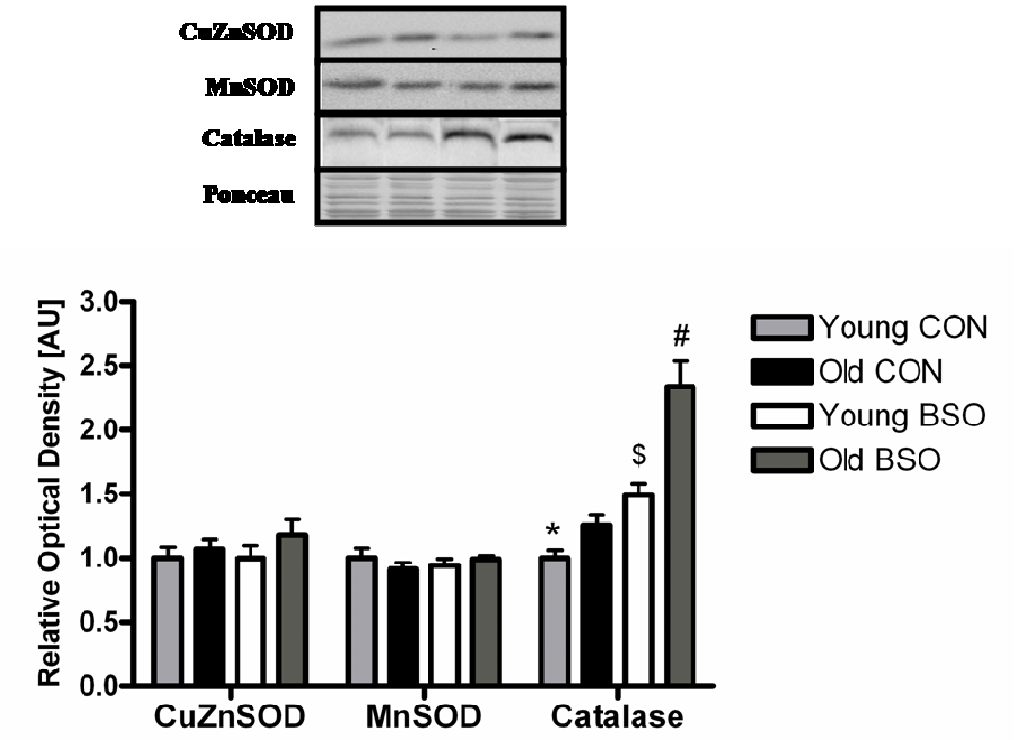

Figure 11: WG antioxidant protein levels across all 4 experimental groups as assessed by densitometry. Representative immunoblots are shown, with a ponceau image to show equal protein loading; from left to right, lane 1: Young CON, lane 2: Old CON, lane 3: Young BSO, lane 4: Old BSO. All values are relative optical densities normalized to Young CON expressed as means ± SEM. *significantly different than Young BSO and Old BSO ($p<0.05$); **$** significantly different than Young CON and Old BSO ($p<0.05$); **#** significantly different than all other groups ($p<0.05$).

Caspase activity shows differential age-dependent changes in SOL only

In SOL muscle, a main effect for age was observed for caspase-3 activity ($p<0.05$), with 14% higher levels in older compared to younger animals. A similar main effect for age in caspase-8 and caspase-9 activities ($p<0.05$) was observed, with an 18% and 25% increase, respectively, seen in older animals compared to younger counterparts (Figure 12). There was no effect of BSO treatment on these proteolytic enzymes in SOL. Additionally, there was no effect of BSO treatment or age on caspase activation in WG (Figure 13).

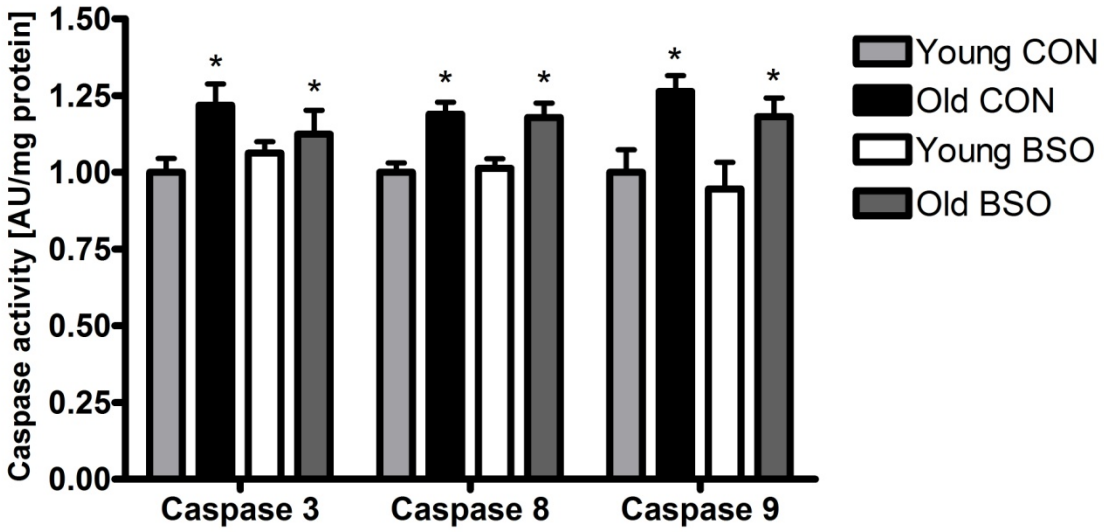

Figure 12: Relative activities for caspases-3, -8, and -9 in SOL muscle; all values are normalized to Young CON group and expressed as means ± SEM. * indicates main effect for AGE ($p<0.05$).

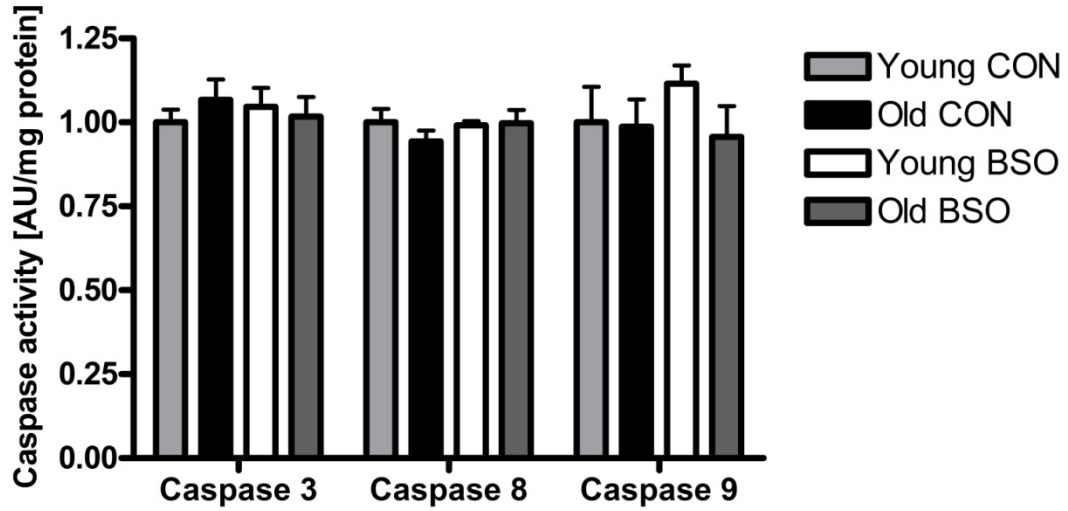

Figure 13: Relative activities for caspases-3, -8, and -9 in WG muscle; all values are normalized to Young CON group and expressed as means ± SEM. **$** significantly different than Young CON and Old BSO ($p<0.05$).

Whole tissue apoptosis-related protein levels demonstrate age-related variations independent of BSO treatment status

Several apoptosis-related proteins were examined in SOL and WG by immunoblot analysis. ARC protein content in SOL was decreased 28% in older animals compared to their younger counterparts ($p<0.05$) while SOL Hsp70 increased 18% in these same animals ($p<0.05$) (Figure 14). Immunohistochemical analysis was also performed for ARC, confirming the above results. Densitometric IHC analysis revealed a 20% decrease in intensity of staining in older SOL muscle cross sections in relation to younger animals (Figure 16, panels B and C). A significantly ($p<0.05$) increased staining intensity in SOL muscle cross-sections was observed compared to WG muscle, with all groups displaying up to a 2-fold higher staining (Figure 16, panels A and B). The only exception was the Old BSO group, whereby the SOL and WG staining intensities were not significantly different (Figure 16 panel C). Lastly, SOL Bcl-2 protein levels did not change significantly from group to group (Figure 14).

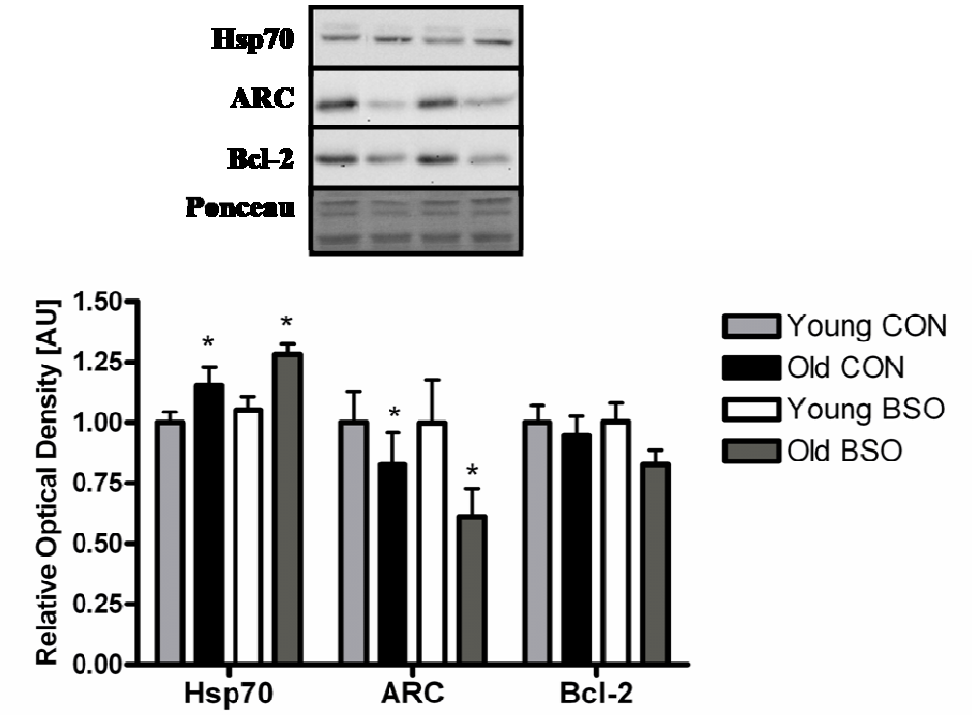

Figure 14: SOL anti-apoptotic protein levels for all experimental groups as assessed by densitometry. Representative immunoblots are shown, with a ponceau image to show equal protein loading; from left to right, lane 1: Young CON, lane 2: Old CON, lane 3: Young BSO, lane 4: Old BSO. Data are presented as relative optical densities normalized to Young CON and expressed as means ± SEM. *indicates main effect for AGE ($p<0.05$).

In contrast, there were no significant changes in Hsp70 protein expression in WG muscle (Figure 15). A significant interaction ($p<0.05$) revealed decreased ARC protein levels in the Young BSO group compared to the Young CON in WG, with no other differences observed. The WG immunohistochemical staining results were not significant.

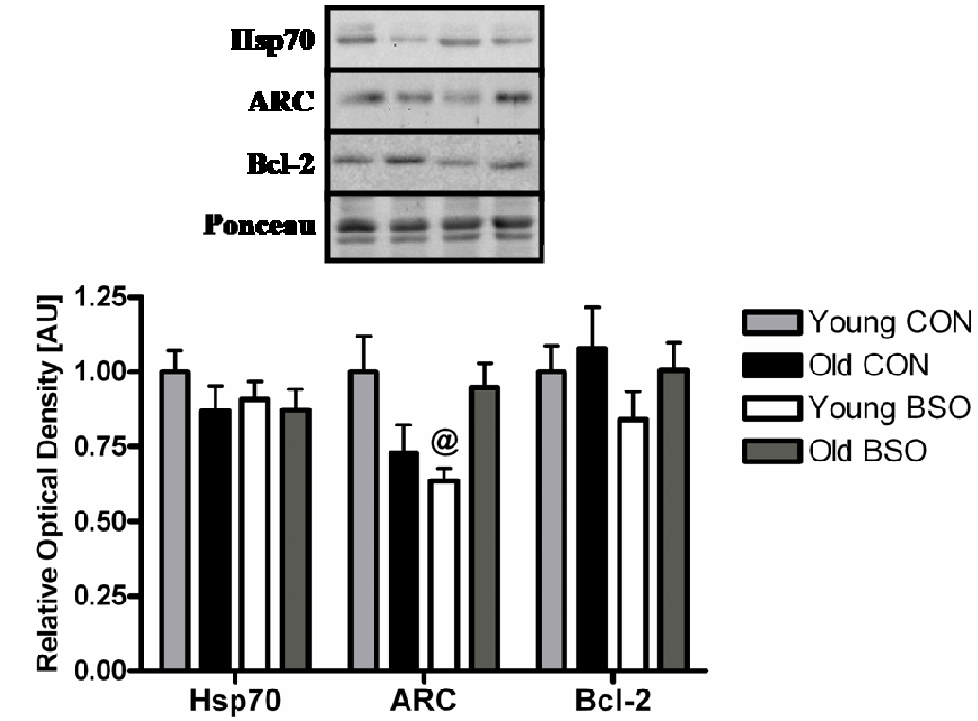

Figure 15: WG Hsp70 and ARC protein levels for all experimental groups as assessed by densitometry. Representative immunoblots are shown, with a ponceau image to show equal protein loading; from left to right, lane 1: Young CON, lane 2: Old CON, lane 3: Young BSO, lane 4: Old BSO. Data are presented as relative optical densities normalized to Young CON and expressed as means ± SEM. @ significantly different than Young CON ($p<0.05$).

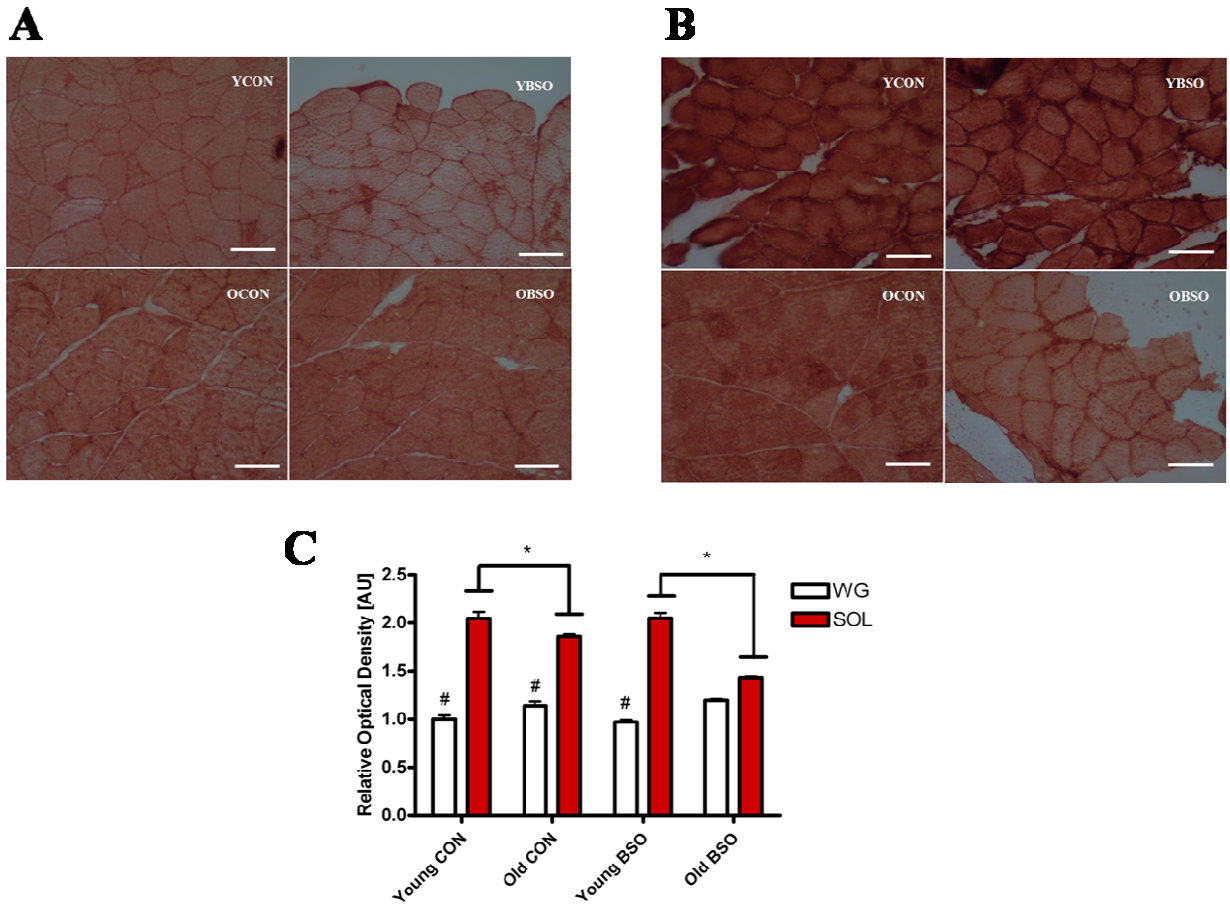

Figure 16: Results of immunohistochemical staining and densitometric analysis of muscle sections from all experimental groups. Panel A contains the representative photomicrographs of WG ARC staining; Panel B contains the representative photomicrographs of SOL ARC staining. Scale bar = 100μm. YCON: Young CON; YBSO: Young BSO; OCON: Old CON; OBSO: Old BSO. Panel C contains the densitometric analysis of the immunohistochemical staining. Values are normalized to WG Young CON and expressed as means ± SEM. *indicates a main effect for AGE ($p<0.05$); #significantly different than corresponding SOL value ($p<0.05$).

Pro-apoptotic proteins AIF, Smac and cytochrome c were examined due to their established roles in mitochondria-mediated apoptotic signaling. In SOL and WG, whole-tissue AIF levels did not change as a result of age or BSO treatment (Figures 17 and 18, respectively). In SOL muscle, Smac protein levels decreased 18% in older compared to younger animals ($p<0.05$) (Figure 17). SOL cytochrome c protein levels displayed a significant ($p<0.05$) age-related decrease of up to 30% in old compared to young animals (Figure 17). There were no significant effects observed in WG tissue for Smac protein expression, however, two noteworthy trends did emerge. First, there was a trend ($p=0.10$) toward an increased

expression in aged animals which was primarily due to the high values observed in the Old BSO group (Figure 18). Secondly, there was another nonsignificant trend (p=0.068) towards an interaction effect, again likely due to the higher level of Smac detected in the Old BSO group. WG whole-tissue cytochrome c levels were not significantly different between groups, though a nonsignificant trend (p=0.099) in the interaction term was observed. This was due to the combination of the higher values observed in the Young BSO and the Old CON groups and the lower values in the Young CON and Old BSO groups (Figure 18). Lastly, Bax protein levels, a pro-apoptotic member of the Bcl-2 family of proteins, were examined in both tissues. There were no significant changes measured in either tissue (Figure 17 for SOL, Figure 18 for WG).

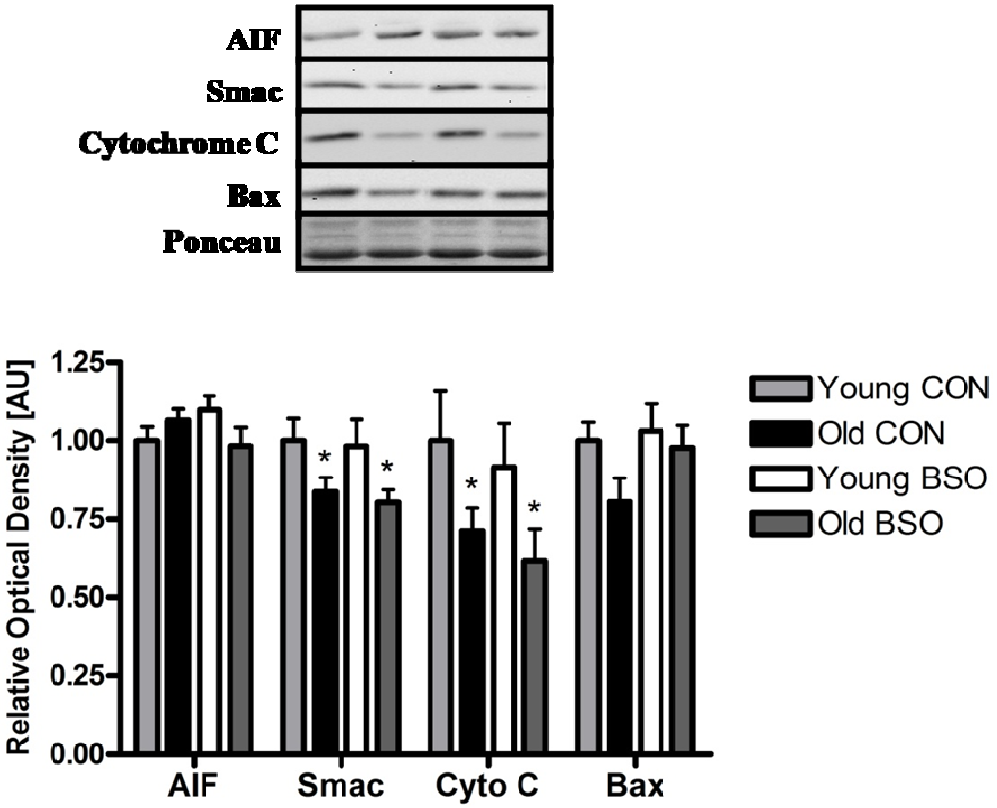

Figure 17: SOL whole-tissue mitochondrial/proapoptotic protein levels for all experimental groups as assessed by densitometry. Representative immunoblots are shown, with a ponceau image to show equal protein loading; from left to right, lane 1: Young CON, lane 2: Old CON, lane 3: Young BSO, lane 4: Old BSO. Data are presented as relative optical densities normalized to Young CON and expressed as means ± SEM. *indicates main effect for AGE ($p<0.05$).

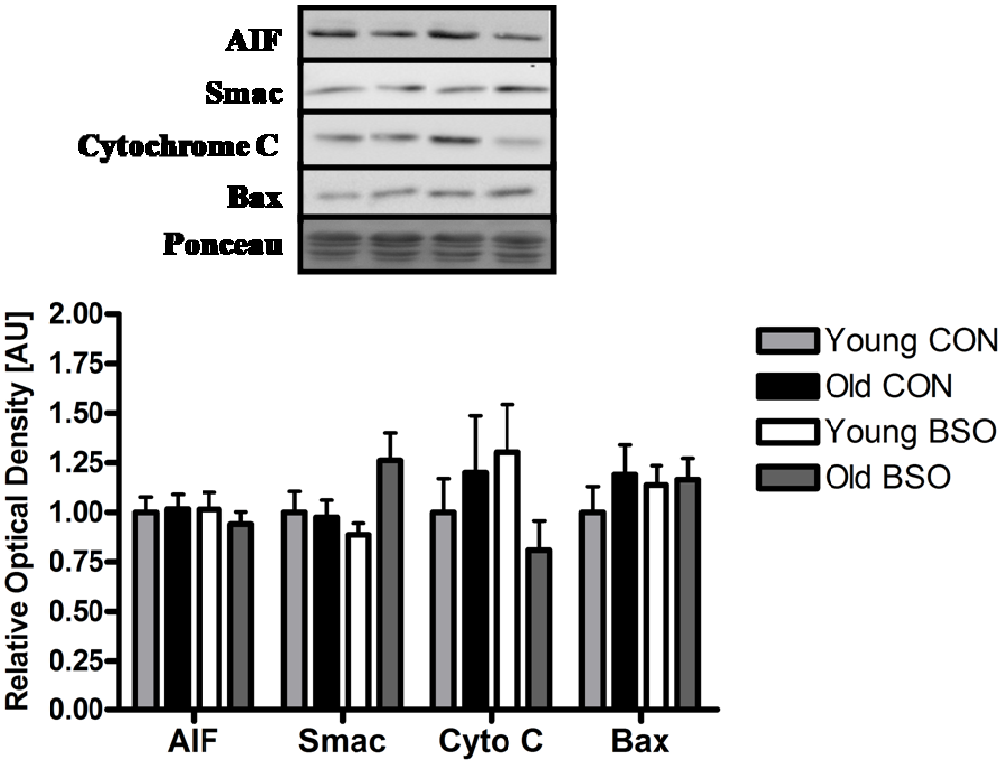

Figure 18: WG whole-tissue mitochondrial/proapoptotic protein levels for all experimental groups as assessed by densitometry. Representative immunoblots are shown, with a ponceau image to show equal protein loading; from left to right, lane 1: Young CON, lane 2: Old CON, lane 3: Young BSO, lane 4: Old BSO. Data are presented as relative optical densities normalized to Young CON and expressed as means ± SEM.

Decreased AIF in cytosolic and nuclear fractions of older animals in WG only

Subcellular fractionation was performed to indirectly examine mitochondrial release of apoptotic proteins such as AIF, Smac and cytochrome c. Three different fractions were isolated from each sample and the relative levels of the apoptotic proteins of interest were determined. In the cytosolic fraction, AIF, Smac and cytochrome c were investigated while in the nuclear fraction, only AIF levels were determined. The mitochondrial fraction was not used in these analyses. All three fractions were, however, used to verify the purity of the obtained subcellular fractions by blotting for fraction-specific proteins. As seen in Figure 19, CuZnSOD was used to assess cytosolic fraction purity, ANT for mitochondrial fraction purity, and histone H2B for nuclear fraction purity.

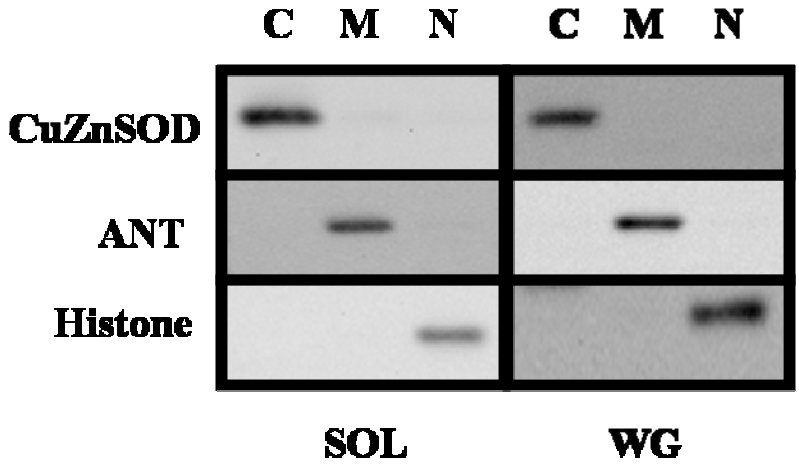

Figure 19: Representative immunoblots to determine subcellular fraction purity in SOL and WG. "C" denotes the cytosolic fraction, for which CuZnSOD was used to verify purity. "M" denotes the mitochondrial fraction, for which ANT was used to verify purity, and "N" denotes the nuclear fraction, using Histone H2B to verify purity.

In the nuclear fraction, where AIF may translocate to the nucleus to cause caspase-independent apoptosis and DNA fragmentation, AIF protein expression was significantly ($p<0.05$) decreased in aged animals in WG only (Figure 20). WG cytosolic AIF levels followed a similar expression pattern, whereby older animals experienced significantly ($p<0.05$) decreased AIF protein content compared to their younger counterparts (Figure 20). However, in SOL tissue, no significant changes in AIF were observed as a result of either age or BSO treatment (Figure 20). Cytosolic Smac and cytochrome c levels were not significantly altered as a result of BSO treatment or age in either tissue (Figure 21 for SOL, Figure 22 for WG). However, there was a nonsignificant trend ($p=0.094$) towards a 15% decrease in cytosolic cytochrome c in the SOL of older animals (Figure 21).

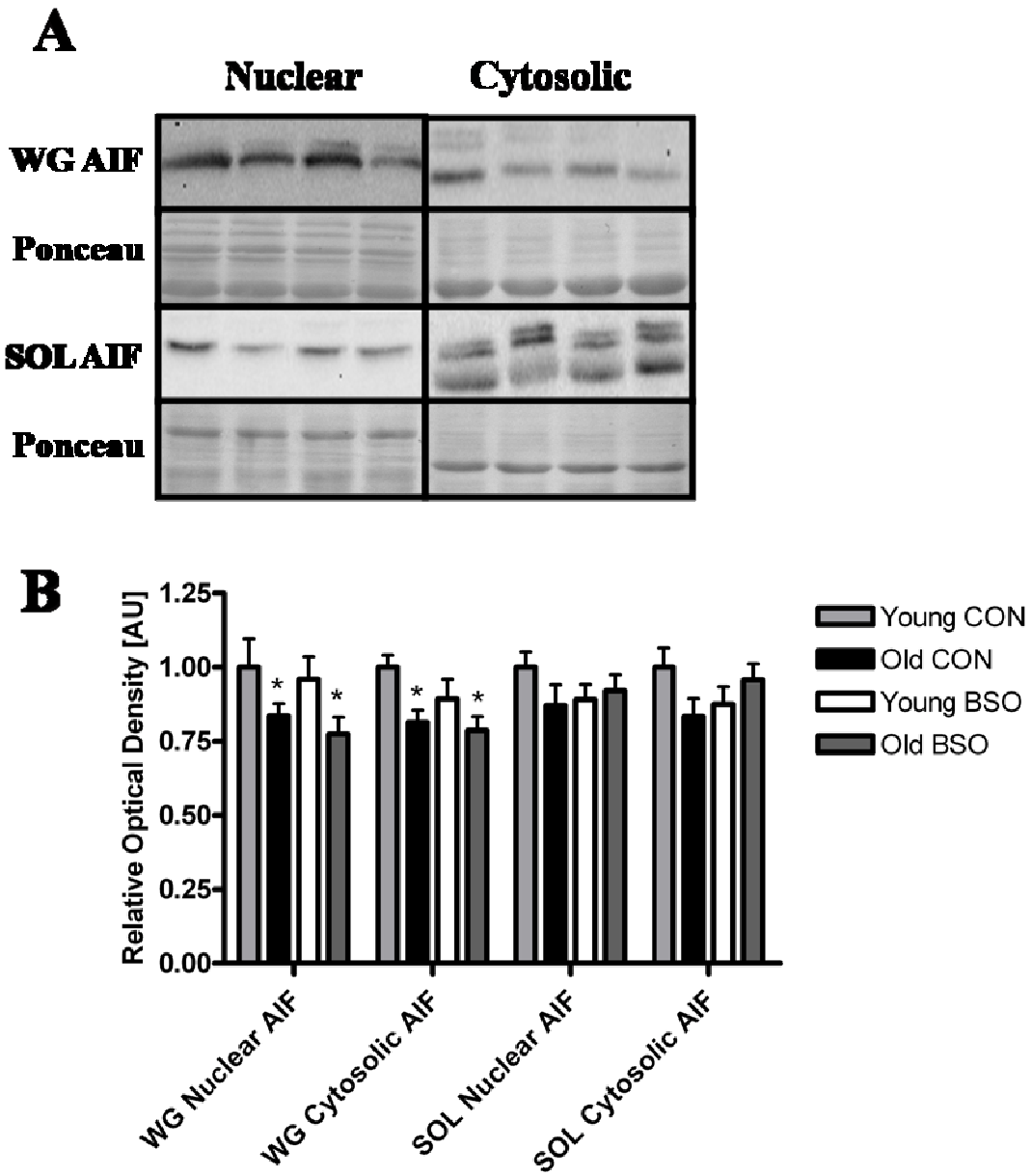

Figure 20: Evaluation of cytosolic and nuclear AIF in WG and SOL. Panel A contains t he representative immunoblots and ponceau images for cytosolic and nuclear AIF in both tissue types; from left to right, lane 1: Young CON, lane 2: Old CON, lane 3: Young BSO, lane 4: Old BSO. Panel B is the densitometric analysis of respective immunoblots. Data are presented as relative optical densities normalized to Young CON for each tissue and expressed as means ± SEM. * indicates main effect for AGE ($p<0.05$).

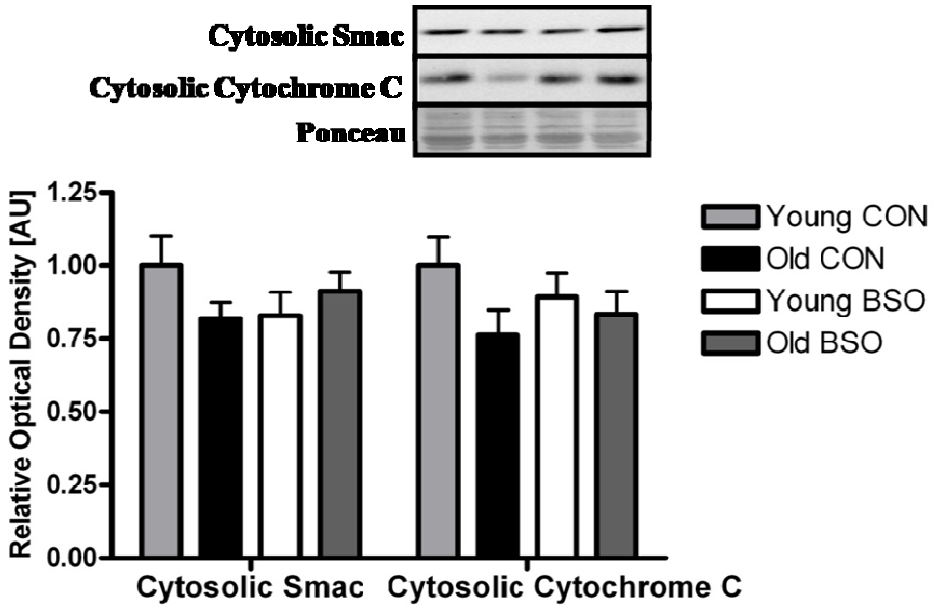

Figure 21: Evaluation of cytosolic Smac and cytochrome c in SOL. Representative immunoblots are shown, with a ponceau image to show equal protein loading; from left to right, lane 1: Young CON, lane 2: Old CON, lane 3: Young BSO, lane 4: Old BSO. Data are presented as relative optical densities normalized to Young CON and expressed as means ± SEM.

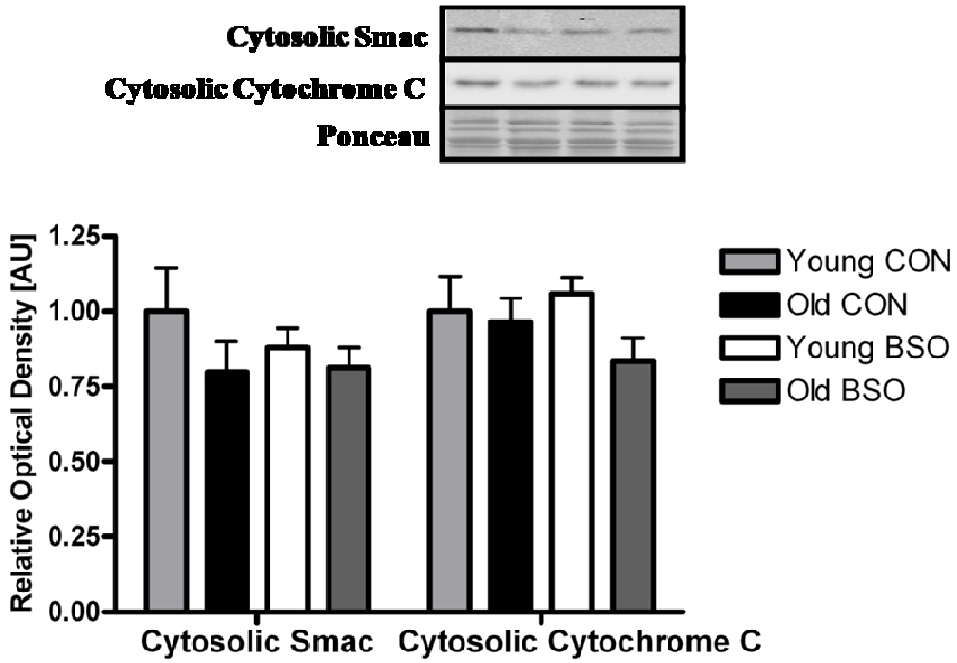

Figure 22: Evaluation of cytosolic Smac and cytochrome c in WG. Representative immunoblots are shown, with a ponceau image to show equal protein loading; from left to right, lane 1: Young CON, lane 2: Old CON, lane 3: Young BSO, lane 4: Old BSO. Data are presented as relative optical densities normalized to Young CON and expressed as means ± SEM.

BSO treatment leads to significant DNA fragmentation in WG with little effect in SOL

DNA fragmentation, one of the hallmark events in apoptosis, was quantified using a Cell Death Detection ELISA. Average DNA fragmentation was increased 38% ($p<0.05$) in BSO-treated animals in WG tissue and 11% ($p<0.05$) in SOL tissue (Figure 23). No age-related changes in DNA fragmentation were observed in either tissue. In addition, DNA fragmentation values were 12-fold higher in SOL tissue compared to WG ($p<0.05$; Figure 23).

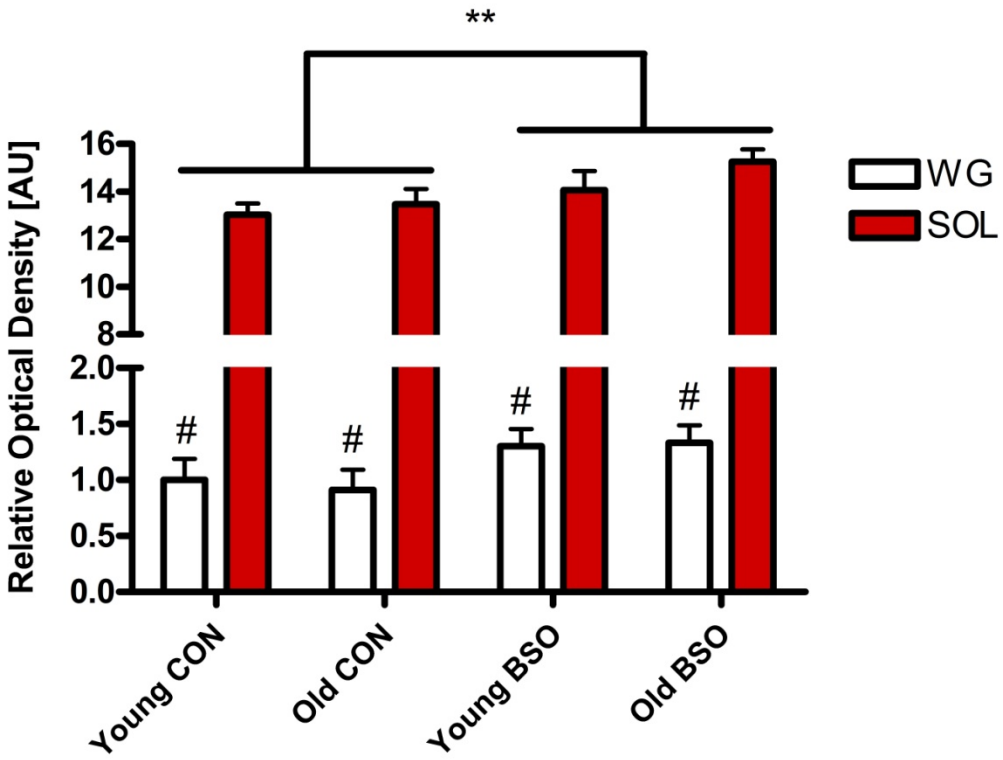

Figure 23: Quantification of DNA fragmentation in SOL and WG tissues using the Cell Death Detection ELISA^{PLUS}. Data shown are relative optical densities normalized to WG Young CON; values are presented as means ± SEM. **indicates the main effect for BSO treatment ($p<0.05$), detected in both SOL and WG tissues; # indicates a main effect for Tissue type ($p<0.05$).

DISCUSSION

Effect of BSO treatment and age on cellular thiol levels and anthropometric indicators

As reported elsewhere,[132, 136, 138, 139, 152, 159, 160, 161] BSO treatment leads to significant reductions in GSH content. In the present work, SOL GSH levels were decreased by 89% compared to age-matched controls, while WG GSH levels were decreased by 96% in the BSO-treated groups. GSH levels were not affected by age in SOL or WG. GSSG levels were decreased as a result of BSO treatment in WG and SOL. Interestingly, in SOL, GSSG levels in the Old CON group were 29% higher than in the Young CON group. GSSG levels were not different due to age in WG. Owing to the fact that GSSG is the oxidized form of GSH, its levels are shown to increase in situations of oxidative stress such as aging.[76] The loss of GSSG observed in this study is primarily due to the severe BSO-induced reduction in GSH synthesis;[137] with very little GSH remaining in the cells, the levels of GSSG are decreased accordingly. There is also some evidence that GSSG can be released from the cell in response to oxidative stress.[162] In other words, when there is less of the oxidized glutathione form (GSSG) present in the cell, the overall GSH:GSSG ratio will be higher. Higher GSH:GSSG ratios are generally indicative of a more reducing environment, which is the "usual" state of the cell.[163] In the present work, these ratios were significantly decreased in SOL and WG as a result of BSO treatment, indicating a shift towards a more oxidative cellular environment.

Interestingly, anthropometric measures were also altered in response to BSO treatment. Animals receiving BSO had significantly lower post-treatment body weights than age-matched controls and experienced greater weight loss over the course of the experimental period. Additionally, there were negative correlations between BSO dose (calculated based on water

intake) and post-treatment body weight and kidney weight. The inverse dose-kidney weight relationship may be indicative of potential drug-induced toxicity, as changes in kidney weight are a commonly-used marker of toxicity.[164] It is possible that potential drug toxicity was a result of the dosage used. In this study, 30mM BSO was used when a more typical dose, as cited in the literature, is 20mM or less.[131, 137, 138, 140] However, there is some debate as to whether the 30mM BSO dose is in fact toxic. Some investigators have observed decreased liver weights, another index of potential drug toxicity, when using the 30mM dose over 14 days[139] while others have observed little to no toxic effects.[165, 166] Tissue damage or other markers of toxicity, such as change in liver weight or liver enzyme activity, would have been helpful to further elucidate the potential toxic effects of BSO; however, these were not performed. Increasing age had an impact on food intake and anthropometric measures, particularly those related to body and organ weight. Older animals consumed less food than their younger counterparts, with the overall lowest food intake seen in the Old BSO group. Body weight was higher in older animals both before and after the BSO treatment, with greater changes in body weight over the 10-day experimental period observed in the old animals compared to the young. Kidney weight was also increased with age.

Measurements of muscle wet weight are typically performed in comparative studies such as this, but unfortunately were not carried out here. In place of this, muscle cross-sectional area (CSA) was used as an approximate indicator of muscle size. Although muscle weights would have been useful, we were interested in studying the SOL and WG muscles specifically. Tissue weight for the SOL would have been easily obtained without any major limitations; however, accurate weight for WG would have been problematic as the isolation of this muscle is somewhat subjective. Measurement of fiber CSA is one way to overcome this

limitation. Muscle wet weight and CSA are typically examined together, particularly in studies focused on aging or muscle atrophy and are nicely correlated.[71] In the WG, CSA was decreased by 16% with age, while in aged SOL, muscle CSA increased by 15%. This selective muscle fiber atrophy is a common observation in experimental aging models. Human gastrocnemius muscle shows decreased type IIA and IIB fiber CSA with age, resulting in an overall decreased muscle size.[167] In addition, the CSA of type I fibers has been shown to vary little, if at all, with age.[167] The differences observed between SOL and WG are interesting but may reflect differences in muscle recruitment. The soleus is a postural muscle composed of primarily type I fibers that is continually recruited, whereas the WG is composed of predominantly type IIB fibers that have a higher recruitment threshold.[168] Therefore, SOL muscle of aged animals may have experienced greater recruitment than WG, coupled with the increased load (body weight), which could have led to selective muscle fiber hypertrophy in the SOL. No BSO-induced changes in fiber CSA area were observed in this study.

Effect of BSO treatment and age on markers of oxidative stress and antioxidant content in WG

To further evaluate the effect of age and BSO on the redox state in the muscle, ROS generation, 4HNE levels and several antioxidant proteins (catalase, MnSOD, CuZnSOD) were measured. In WG, no significant differences in ROS production (as determined by DCFH oxidation) in whole muscle homogenate were observed due to BSO treatment or age. Similarly, 4HNE levels (a measure of lipid peroxidation) were unchanged in the WG across all groups. Furthermore, there were no significant changes observed in the protein content of MnSOD and CuZnSOD irrespective of age or BSO treatment in WG. In contrast, catalase protein content was increased on average by 1.5-fold in older animals and by 1.7-fold in WG of BSO-treated animals. This upregulation, particularly in the BSO-treated group, is noteworthy due to the

similarities between the methods of action of catalase and thiol-dependent glutathione peroxidase (GPx). Catalase is a potent detoxifier of cellular H_2O_2.[117] GPx is another detoxifier of cellular H_2O_2 that consumes 2 GSH molecules in this process.[29] Several studies suggest that the activation of these antioxidant enzyme systems may differ depending on the oxidative stress signal, even though they accomplish similar functions in the cell. For example, paraquat (a potent ROS producer) has been shown to deplete GSH levels while simultaneously increasing SOD and catalase expression and activity without affecting GPx activity.[169] The authors of this work postulate that the depleted GSH levels result in the lack of change in GPx activity, resulting in a reliance on other antioxidant enzymes to combat the oxidative stress.[169] It has also been shown that catalase and GPx activities vary differentially depending on cellular localization of the oxidative stress, with GPx responsible for H_2O_2 generated in the endoplasmic reticulum and catalase handling peroxisomal H_2O_2.[170] Therefore, a compensatory increase in catalase likely occurred as a result of GSH depletion in WG. A compensatory antioxidant upregulation is frequently observed with advancing age, consisting of elevated activity of MnSOD and catalase[77, 171] as well as CuZnSOD and GPx.[171] This upregulated response has also been observed with BSO treatment, consisting of increased activity and content of SOD's in certain tissues such as rat heart and aorta.[82, 159] Lastly, others have shown BSO does indeed lead to decreased activity of GPx1.[82] It is possible that the upregulation in catalase observed with BSO and age was sufficient to maintain ROS and lipid peroxidation at levels similar to the Young CON animals.

Effect of BSO treatment and age on markers of oxidative stress and antioxidant content in SOL

In contrast to the WG muscle, SOL displayed a 20% increase in ROS production due to BSO treatment with no independent effect of age. The higher ROS in SOL of BSO-treated animals

with no observable difference in WG may be a consequence of the different ROS sources between tissues. It is well-documented that SOL has a high mitochondrial content compared to WG.[172, 173, 174] For example, markers of mitochondrial content such as citrate synthase activity are 2.6-fold higher in SOL compared to WG,[174] while succinate dehydrogenase activity is 2.2-fold higher in SOL.[173] Results from our lab are consistent with these findings (Bloemberg & Quadrilatero, 2010). Other markers of mitochondrial density, such as PGC-1α protein levels, are elevated in SOL compared to WG in the basal state.[172] In addition, mitochondria are a significant source of ROS,[86, 87, 89] meaning they may require increased defense against oxidative damage. As such, there is a distinct mitochondrial pool of GSH[134] and work in our lab has shown that GSH is depleted in isolated mitochondria of BSO-treated animals (Dam et al., 2010). Accordingly, the higher ROS in the SOL of BSO-treated animals could be attributed to elevated ROS production from sources such as the mitochondria. In contrast, there were no age effects seen in ROS production. The lack of an age effect in SOL and WG may be due to the fact that the aged animals used in this study (ie. 17 months old) were not as old as those typically used in aging research (24-36 months old). This is supported by work conducted in rat muscle examining measures of oxidative protein damage in young (5 months), adult (13 months) and old (24 months) animals.[175] Oxidative damage markers such as protein carbonyls and nitrotyrosine were only increased in the oldest compared to the youngest group, with no elevation in the adult age group.[175] These results may indicate that the mid-range age of our "old" animals may not have been sufficient to observe the usual age-related changes in oxidative stress.

SOL 4HNE levels showed a slight decrease in BSO animals compared to controls with no age-related effect observed. This result conflicts with the observed increase in ROS

production due to BSO treatment. Higher ROS production would be expected to lead to increased markers of lipid peroxidation including 4HNE.[176] There is some evidence that the levels of 4HNE may intimately depend on cellular GSH concentration, whereby the 4HNE produced when cells are GSH-depleted may actually be more easily metabolized and broken down.[177] Another perspective is the fact that a major route of 4HNE detoxification is through conjugation with GSH via the class of enzymes known as glutathione-*S*-transferases (GST).[178] Interestingly, it was found that 14 days of 30mM BSO treatment leads to paradoxically increased tissue GST activity.[139] Therefore, it is possible an increased GST activity in BSO animals could lead to increased clearance of the 4HNE peroxidation product. This, in turn, could explain the decreased signal for 4HNE in our BSO-treated animals in the SOL. Quantification of GST protein and activity levels would be necessary to clarify this point; however, these analyses were not performed in the present work. There was no difference in CuZnSOD or MnSOD content as a result of age or BSO treatment. However, SOL catalase protein expression was substantially upregulated by 1.5-fold in older and 1.5-fold in BSO-treated animals. This upregulated antioxidant defense is likely a compensatory effect that would serve to aid in muscle clearance of H_2O_2 in the absence of GSH as noted above. The reason for the differential response in ROS generation observed in SOL compared to WG following BSO treatment are unclear but may reflect a higher "oxidative environment" of the SOL,[179, 180] which could have been augmented in a GSH-depleted state. For instance, malondialdehyde levels (MDA, a marker of lipid peroxidation) are higher in the SOL muscle compared to vastus lateralis in rats; additionally, enzyme activity for several antioxidants such as SOD, GPx and catalase are comparably elevated in the SOL.[179] Other groups have shown similar results in terms of lipid peroxidation markers and antioxidant enzyme activity, and have

also demonstrated increased markers of mitochondrial density in SOL compared to less oxidative muscles such as red gastrocnemius or WG.[180]

Effects of BSO treatment and age on apoptotic signaling in WG

In the present investigation we found a 38% higher level of DNA fragmentation in WG of BSO-treated animals compared to untreated controls. In contrast, no differences in DNA fragmentation were observed in WG of older compared to younger animals. In addition, there were no significant differences in caspase-3, -8, or -9 activity between groups. The elevated DNA fragmentation in the absence of increased caspase activity in BSO-treated animals is surprising but could suggest that caspase-independent mechanisms are playing a role. For example, AIF and EndoG are two mitochondrial proteins that can lead to DNA fragmentation independent of caspase activation.[32, 45] However, as discussed below, AIF-mediated signaling is likely not involved as we found decreased levels in cytosolic and nuclear fractions. It is possible that EndoG (or other factors) may have played a role in the observed effect; however, this remains to be determined. It is also possible that the increased rate of DNA fragmentation observed in BSO animals is attributable to other sources of nuclear material outside of myonuclei (ie. interstitial cells, macrophages).[57, 181] Using TUNEL staining (a microscopic method which stains for fragmented DNA in muscle cross-sections) in a rabbit model of limb immobilization, Smith and colleagues reported that the majority of TUNEL-positive cells observed were outside of the outline of muscle fibers.[181] A similar study using limb unweighting in rats showed that most TUNEL-stained nuclei were located in the interstitium or in connective tissue bands.[57] In the present work, DNA fragmentation was only assessed using whole muscle homogenates, without the added compliment of TUNEL staining. Given that any

apoptotic interstitial or immune cells located in the muscle homogenate would be indiscernible from apoptotic myonuclei, the level of DNA fragmentation may have been overestimated.

The lack of DNA fragmentation in WG of older animals is somewhat surprising; however, a closer examination of the literature may explain this finding. Previous work has shown an age-related increase in muscle apoptosis;[64, 71, 73, 182] however, this is heavily dependent on the age of experimental animals. For example, Marzetti and colleagues have shown that DNA fragmentation in rat gastrocnemius muscle is not elevated in 18 month-old animals compared to adults (8 months), but is significantly increased at 29 months of age and older.[183] This group also shows no change in several other apoptotic markers, such as Bax, active caspase-9, or mitochondrial Bid, between 8- and 18-month old animals.[183] Similarly, the decrease in fiber CSA in the absence of increased DNA fragmentation in WG in older animals is also puzzling. However, recent advances in time-lapse microscopy have shown that CSA of fibers decreases in the absence of apoptotic nuclei during disuse atrophy.[184] Atrophy and loss of muscle mass have been associated with the ATP-dependent ubiquitin-proteasome pathway of protein degradation, a process that may occur in the absence of classical markers of apoptosis (ie. DNA fragmentation).[185] Tawa and colleagues have demonstrated attenuation of muscle wasting due to treatment with drugs that inhibit the proteasome, accompanied by decreased protein ubiquitination.[186] In addition to the potential increased activity of this degradation pathway, aging muscle also displays decreased protein synthesis.[187] Therefore, it is possible that a protein degradation pathway combined with decreased protein synthesis is involved in the atrophy observed in WG that is independent of apoptotic signaling. However, measures of proteasome activation, protein ubiquitination and protein synthesis were not performed in the present work.

Several anti-apoptotic proteins were also measured in WG muscle. Immunoblot analysis revealed no differences in both Hsp70 and Bcl-2 protein content across all groups. There was, however, a significant interaction in ARC protein with lower levels in the Young BSO compared to the Young CON. However, IHC analysis showed no significant differences in ARC protein between groups. This result is anomalous as there were no BSO-specific decreases in ARC observed in the Old groups. It is currently unclear what accounts for these differences.

In general, we found very few changes in the level of several pro-apoptotic proteins in WG muscle between groups. For example, whole muscle Bax, Smac, AIF, and cytochrome c were all unchanged due to age or BSO treatment. Furthermore, there were no significant differences in the levels of cytosolic Smac or cytochrome c between all groups. In contrast, cytosolic and nuclear AIF were decreased in old animals, with no differences in response to BSO treatment. Siu and colleagues also found decreased nuclear AIF in aged mixed gastrocnemius muscle along with no change in cytosolic AIF levels and increased whole-tissue expression of this protein;[188] however, the underlying reason for these findings was unclear. Collectively, the results of the current study suggest that the degree of aging in the animals used in this study was not sufficient to induce apoptosis but may be sufficient to induce a protein degradation pathway of muscle loss.

Effects of age and BSO treatment on apoptotic signaling in SOL

DNA fragmentation in SOL muscle was significantly elevated in BSO-treated animals compared to controls with no age-related changes noted in this measure. However, activity measures for three major caspases (caspase-3, -8, and -9) showed age-related differences, with

higher proteolytic activity found in older animals. The activity of these caspases was not different between groups in response to BSO treatment. This is somewhat puzzling given the role of caspases in apoptosis and DNA fragmentation. However, there is evidence that caspases do not exclusively function in apoptotic signaling (though that is their primary function). Recent work shows that caspase-3 and its downstream cleavage product caspase-activated DNase promote skeletal muscle cell differentiation by inducing essential DNA strand breaks in the terminal step of this process.[189] Other groups have shown that myoblasts exposed to caspase-3 and caspase-8 inhibitors are unable to differentiate.[190] This could be a reason for the increased caspase activation observed in aged SOL in the absence of DNA fragmentation. More specifically, given the higher muscle weights in old SOL, it is possible that activation of satellite cells (myoblasts) was increased. These myoblasts proliferate, differentiate and then incorporate into the muscle fiber to aid in muscle hypertrophy.[191] Therefore, the increased caspase activity seen here may reflect a shift towards increased muscle regeneration in this tissue through induction of satellite cell differentiation and subsequent proliferation. However, this remains to be determined.

The levels of several anti-apoptotic proteins (Hsp70, ARC, Bcl-2) were not affected by BSO treatment in SOL. Similarly, the levels of Bcl-2 protein were not affected by age. In contrast, Hsp70 protein content was significantly higher in old versus young animals. Interestingly, Hsp70 protein levels mirrored the increase in caspase activity in SOL, highlighting that advancing age may be inducing a state of cellular stress in this tissue.[192] Hsp70 expression has been shown to increase from middle-aged (16-month) to senescent (29-month) rats, with a concomitant increase in cleaved caspase-9.[193] Hsp70 has also been shown to interact with and antagonize Apaf-1, a necessary component of the caspase-9-activating

apoptosome.[194] Some studies have shown that Hsp70 may exert its protective effects downstream of caspase-3 activation,[195] thus allowing other cellular events of the caspase cascade to occur while inhibiting substrate cleavage and apoptotic death. Therefore, although caspase-3 and -9 activity was elevated, the increased Hsp70 content could have been sufficient to inhibit caspase-mediated DNA fragmentation and apoptotic events in older animals.

Several pro-apoptotic proteins were also measured in SOL. Whole muscle AIF and Bax content were not affected by age or BSO treatment. Similarly, whole-tissue Smac and cytochrome c levels were not affected by BSO treatment. In contrast, whole SOL Smac and cytochrome c were significantly decreased in older animals. Although at first glance it would seem that this may be indicative of less apoptosis in aged animals, it is important to note that these proteins are part of the mitochondria and generally have vital functions independent of their role in apoptosis.[196] Release of these proteins from the mitochondrial intermembrane space into the cytosol is essential to their pro-apoptotic function.[32, 33] Further, subcellular distribution studies performed here showed no effects similar to those observed in the whole tissue homogenate. In particular, age had no effect on cytosolic AIF, Smac or cytochrome c, nor on nuclear AIF. Decreased whole-tissue expression of mitochondrial apoptotic factors, in the absence of subcellular changes indicative of mitochondrial release of these apoptogenic proteins, may simply indicate decreased mitochondrial content. There is evidence to show a decrease in mitochondrial density in elderly humans compared to their adult counterparts.[197] Others have shown similar results, whereby mitochondrial content and other measures of mitochondrial density (mtDNA abundance and citrate synthase activity) are decreased in aged patients compared to younger counterparts.[198]

In contrast to the higher Hsp70 levels observed in older animals, anti-apoptotic ARC expression was decreased in SOL of older animals as assessed by both immunohistochemical analyses and immunoblot analysis. Similarly, Siu and Alway have demonstrated decreased expression of anti-apoptotic factors (ie. ARC, XIAP) and increased H_2O_2 levels in aged muscle after 7 days of loading compared to younger animals.[199] Interestingly, ARC degradation has been shown to occur through the ubiquitin-proteasome in response to such cellular stress.[6, 99] Collectively, this ARC data along with the higher Hsp70 levels suggest that SOL muscle of older animals may have been under greater stress. However, this stress was not sufficient to increase DNA fragmentation (apoptosis) or muscle wasting.

The data presented herein for WG and SOL suggest differential apoptotic effects due to BSO treatment and/or age. In WG, loss of muscle mass is apparent even in the absence of elevated apoptotic signaling while this trend does not hold in SOL. BSO-induced DNA fragmentation is observed in conjunction with oxidative modifications as assessed by GSH depletion and catalase upregulation in both tissues examined.

Several tissue-specific changes were observed in this study

There were several noteworthy differences observed between the two muscles tested in this study. As alluded to in the previous discussion, the higher mitochondrial volume of SOL compared to WG may result in increased ROS production. Although a direct analysis of mitochondrial volume or content was not performed between these two muscles, the differences are obvious when examining the absolute ROS production (Figure 7 in Results). Specifically, a substantially higher level of ROS production was observed in the slower, more oxidative SOL compared to the faster, more glycolytic WG. In support of this observation,

higher 4HNE immunofluorescent staining was seen in the more oxidative SOL muscle compared to the more glycolytic WG. This is consistent with reports indicating that malondialdehyde (MDA, a marker of lipid peroxidation) content was substantially increased in SOL muscle compared to WG.[180] In addition, the 4HNE staining pattern observed between SOL and WG was very distinct: in WG more whole-fiber staining occurred, with smaller fibers more intensely stained than larger fibers. It is likely that these smaller fibers represent IIXB or IIX fibers, which are smaller than IIB[200] (Bloemberg & Quadrilatero, 2010). Interestingly, IIX and IIXB fibers would tend to have a higher oxidative potential and therefore, mitochondrial content[200] (Bloemberg & Quadrilatero, 2010). In the SOL, the cell membranes were more heavily stained compared to the inside of the fibers. The SOL staining pattern observed may be explained by the fact that 4HNE would be more likely to be found on or around the plasma membrane, due to the high concentration of polyunsaturated fatty acids which would be more susceptible to lipid peroxidation, ensuing radical chain reactions and formation of 4HNE adducts.[176] In further support of the more oxidative environment of SOL muscle, both GSH and GSSG levels were found to be significantly higher in this muscle than WG. In fact, SOL GSH was higher than WG GSH across all groups including the BSO-treated groups. A similar trend persisted in terms of GSSG levels whereby SOL had consistently higher levels of GSSG across all groups compared to the same groups in WG. Similarly elevated basal GSH levels in oxidative muscles like SOL have been observed by others compared to more glycolytic muscles.[179, 201]

DNA fragmentation levels were up to 12-fold higher in SOL compared to WG. Combined with the increased markers of oxidative stress in this muscle, this piece of data lends support to the link between oxidative stress and apoptotic signaling.[75, 98] SOL also experiences

a 2-fold higher intensity of ARC staining compared to the more glycolytic WG that, when taken together with the increased DNA fragmentation rates observed, may be indicative of a protective mechanism developed by the muscle against endogenous damage. Our lab has observed similar increases in anti-apoptotic ARC protein expression in red gastrocnemius muscle compared to WG (McMillan & Quadrilatero, 2010). We have also shown elevated Hsp70 protein expression in slower muscle compared to fast, an observation consistent with the fiber-type specific expression of Hsp70.[202] Slow muscles have higher protein levels of Bcl-2 compared to their fast counterparts (McMillan & Quadrilatero, 2010). Lastly, slower muscles vary from their faster counterparts on other important markers of muscle health such as higher protein synthesis rates[203] and increased satellite cell numbers associated with slow muscle fibers.[204]

CONCLUSIONS

The purpose of the present study was to explore the effects of glutathione depletion by BSO on apoptotic signaling in different types of young and old skeletal muscle. Apoptosis, as assessed by DNA fragmentation, was elevated in both the WG and SOL tissue due to BSO treatment. However, in WG this occurred in the absence of other pertinent markers of apoptotic signaling (ie. nuclear AIF translocation, increased caspase activity, mitochondrial release of Smac/cytochrome c, increased Bax, or decreased Bcl-2, ARC, Hsp70). No potent effects of aging were observed in the WG muscle other than loss of muscle mass as assessed by decreased muscle CSA. While the lack of DNA fragmentation and elevated apoptotic signaling in this tissue are contrary to the established literature, a possible explanation is offered by the fact that our old animals were not aged sufficiently to produce such effects. However, the age of the experimental animals offers an interesting perspective for examining the effects of in vivo antioxidant depletion. In other words, given the lack of change in basal GSH content in the Old CON animals compared to the Young CON, use of a chemical depletion model in addition to these age groups may show additive effects that could otherwise be lost in a model of advanced age. In particular, the elevated oxidative stress and apoptotic signaling typical of skeletal muscle from very old animals could confound any further effects of the BSO-induced GSH depletion in this tissue, making the age range of the animals used here useful for capturing any such synergistic effects.

In the SOL muscle, while DNA fragmentation and ROS production increased in BSO-treated animals, a slight decrease in 4HNE levels was observed. This is thought to result from elevated GST activity in these animals, though this point remains to be determined. A potentially elevated stress state may be occurring in aged SOL muscle, as evidenced by

elevated caspase activation and Hsp70 content as well as decreased levels of anti-apoptotic ARC. In addition, aged SOL muscle increased slightly in size in the present study, likely due to the increased body weight of older animals resulting in a greater load for this postural muscle to support as well as possible satellite cell activation. Furthermore, SOL muscle showed increased oxidative stress markers (ROS production and 4HNE levels), elevated DNA fragmentation and expression of ARC protein compared to WG, offering further evidence for the theory of elevated basal cellular stress occurring in more oxidative muscles compared to their more glycolytic counterparts (ie. SOL versus WG). Additionally, GSH and GSSG levels are elevated in SOL compared to WG which, taken together, indicate somewhat higher cellular stress accompanied by a greater antioxidant pool to handle that stress.

Relating the experimental evidence back to the hypotheses postulated for this work, BSO treatment was effective in depleting muscle GSH. However, differential effects were observed in SOL and WG tissue in terms of the postulated increases in ROS production. Aging did not result in the anticipated increase in oxidative stress, nor did there appear to be any additive effect of BSO treatment and age on any measure other than catalase expression. GSH depletion was not sufficient to induce a classical apoptotic phenotype in either muscle type examined. Instead, in WG a process possibly related to a muscle degradation pathway emerged independent of apoptotic cell death with age, while BSO only resulted in disrupted thiol balance and upregulated catalase. In contrast, SOL muscle displayed an elevated state of cellular stress with age, experiencing disrupted thiol balance and only modest elevations in oxidative stress markers due to BSO treatment. Based on these data, BSO-induced GSH depletion does not seem to increase apoptotic signaling in either tissue examined, irrespective of age. The mid-range of the animals in this study helped to highlight the changes in apoptotic

signaling and antioxidant upregulation that occur as animals advance through the aging process.

LIMITATIONS

There were several limitations to this study that are mostly methodological in nature. First, the muscles used were not weighed at the time of isolation, leaving the muscle cross-sectional area as the only estimate of muscle size. Having both CSA and muscle wet weight data could have strengthened the interpretations made herein concerning the observed changes in CSA of WG and SOL. Second, no measurements of GPx or GST activity were performed. These results could have helped clarify the extent to which the thiol system of the cell was impacted by the BSO-induced GSH depletion, or if there were any specific compensatory mechanisms at work as a result of the extreme GSH depletion observed.

Focusing specifically on apoptotic signaling, with the exception of AIF protein levels and subcellular localization, no other measures of caspase-independent apoptosis were performed. In particular, no measure of protein levels or nuclear localization of Endonuclease G was performed. This protein is another important mitochondria-housed factor involved in caspase-independent cell death[45]. TUNEL staining could have helped clarify if the levels of DNA fragmentation observed were due to myonuclear loss or apoptotic processes in other cells present in whole skeletal muscle. Lastly, the idea of degradative mechanisms at work only in WG tissue would require quantification of proteasome activity, as well as measurement of expression for the various components of this cellular machinery.

FUTURE DIRECTIONS

As suggested throughout the discussion section of this thesis, there are several modifications that could have greatly improved the results obtained and that would be good starting points for future directions. Any further work in this area would benefit from examination of GST and GPx expression and enzyme activity quantification, as well as expression and subcellular localization of Endonuclease G. Additionally, while some studies have examined the potentially additive effects of stress (ie. exercise) on GSH-depleted animals[82, 132], the focus on apoptotic effects of this elevated stress state has been absent. It would be interesting to consider young (4-8 months), middle-aged/adult (14-18 months) and old (24 months and above) GSH-depleted and control animals exposed to an eccentric exercise protocol such as treadmill running on a downward incline. In addition, consideration of acute and prolonged exposure to such exercise could clarify potentially protective effects, or demonstrate the additive negative effects of increased activity, lowered thiol content and changes in ROS production of this type of exercise. Since the muscle samples were taken after 10 days of treatment, it could be useful to isolate muscle tissue at different time points in the BSO treatment protocol. There is some evidence that BSO effectively depletes in vivo GSH levels as early as 24 hours after the first administration[133].By examining different time points in a BSO drug treatment, it may be possible to more accurately pinpoint the occurrence of apoptotic signalling events in relation to the level of GSH depletion obtained by the administration of the drug. Furthermore, evaluation of the ubiquitin-proteasome system in the context of BSO-induced GSH depletion in skeletal muscle could offer valuable insight into the potentially adverse whole-body effects of this drug. This would be important as BSO is currently under investigation for its usefulness in cancer therapy.

REFERENCES

1. Majno G, Joris I. Apoptosis, Oncosis, and Necrosis. *American Journal of Pathology*. 1995;146(1):3-15.

2. Glücksmann A. Cell Deaths in Normal Vertebrate Ontogeny. *Biological Reviews*. 1951;26(1):59-86.

3. Taddeo B, Nickoloff BJ, Foreman KE. Caspase inhibitor blocks human immunodeficiency virus 1-induced T-cell death without enhancement of HIV-1 replication and dimethyl sulfoxide increases HIV-1 replication without influencing T-cell survival. *Archives of Pathology & Laboratory Medicine*. 2000;124(2):240-245.

4. Terai C, Kornbluth RS, Pauza CD, Richman DD, Carson DA. Apoptosis as a mechanism of cell death in cultured T lymphoblasts acutely infected with HIV-1. *The Journal of Clinical Investigation*. 1991;87(5):1710-1715.

5. Murtaza I, Wang H, Feng X, et al. Down-regulation of catalase and oxidative modification of protein kinase CK2 lead to the failure of apoptosis repressor with caspase recruitment domain to inhibit cardiomyocyte hypertrophy. *The Journal of Biological Chemistry*. 2008;283(10):5996-6004.

6. Foo RS, Chan LK, Kitsis RN, Bennett MR. Ubiquitination and degradation of the anti-apoptotic protein ARC by MDM2. *The Journal of Biological Chemistry*. 2007;282(8):5529-5535.

7. Efrati S, Berman S, Goldfinger N, et al. Enhanced angiotensin II production by renal mesangium is responsible for apoptosis/proliferation of endothelial and epithelial cells in a model of malignant hypertension. *Journal of Hypertension*. 2007;25:1041-1052.

8. Kedi X, Ming Y, Yongping W, Yi Y, Xiaoxiang Z. Free cholesterol overloading induced smooth muscle cells death and activated both ER- and mitochondrial-dependent death pathway. *Atherosclerosis*. 2009;207:123-130.

9. Quadrilatero J, Rush JW. Evidence for a pro-apoptotic phenotype in skeletal muscle of hypertensive rats. *Biochemical and Biophysical Research Communications*. 2008;368:168-174.

10. Bargou RC, Wagener C, Bommert K, et al. Overexpression of the death-promoting gene bax-alpha which is downregulated in breast cancer restores sensitivity to different apoptotic stimuli and reduces tumor growth in SCID mice. *The Journal of Clinical Investigation*. 1996;97(11):2651-2659.

11. Christensen JG, Romach EH, Healy LN, et al. Altered bcl-2 family expression during non-genotoxic hepatocarcinogenesis in mice. *Carcinogenesis*. 1999;20(8):1583-1590.

12. Strasser A, Harris AW, Jacks T, Cory S. DNA damage can induce apoptosis in proliferating lymphoid cells via p53-independent mechanisms inhibitable by Bcl-2. *Cell*. 1994;79(2):329-339.

13. Kerr JF, Wyllie AH, Currie AR. Apoptosis: a basic biological phenomenon with wide-ranging implications in tissue kinetics. *The British Journal of Cancer*. 1972;26:239-257.

14. Wachstein M, Besen M. Electron microscopy of renal coagulative necrosis due to dl-serine, with special reference to mitochondrial pyknosis. *American Journal of Pathology*. 1964;44(3):383-400.

15. Alnemri ES. Mammalian cell death proteases: A family of highly conserved aspartate specific cysteine proteases. *Journal of Cellular Biochemistry*. 1997;64:33-42.

16. Wolf BB, Green DR. Suicidal tendencies: Apoptotic cell death by caspase family proteinases. *Journal of Biological Chemistry*. 1999;274(29):20049-20052.

17. Wolf BB, Schuler M, Echeverri F, Green DR. Caspase-3 is the primary activator of apoptotic DNA fragmentation via DNA fragmentation factor-45/inhibitor of caspase-activated DNase inactivation. *The Journal Biological Chemistry*. 1999;274(43):30651-30656.

18. Liu X, Zou H, Slaughter C, Wang X. DFF, a heterodimeric protein that functions downstream of caspase-3 to trigger DNA fragmentation during apoptosis. *Cell*. 1997;89(2):175-184.

19. Srinivasula SM, Ahmad M, Fernandes-Alnemri T, Litwack G, Alnemri ES. Molecular ordering of the Fas-apoptotic pathway: the Fas/APO-1 protease Mch5 is a CrmA-inhibitable protease that activates multiple Ced-3/ICE-like cysteine proteases. *Proceedings of the National Academy of Sciences USA*. 1996;93:14486-14491.

20. Takahashi A, Hirata H, Yonehara S, et al. Affinity labeling displays the stepwise activation of ICE-related proteases by Fas, staurosporine, and CrmA-sensitive caspase-8. *Oncogene*. 1997;14:2741-2752.

21. Muzio M, Stockwell BR, Stennicke HR, Salvesen GS, Dixit VM. An induced proximity model for caspase-8 activation. *The Journal of Biological Chemistry*. 1998;273(5):2926-2930.

22. Yang X, Chang HY, Baltimore D. Autoproteolytic activation of pro-caspases by oligomerization. *Molecular Cell*. 1998;1:319-325.

23. Butt AJ, Harvey NL, Parasivam G, Kumar S. Dimerization and autoprocessing of the Nedd2 (caspase-2) precursor requires both the prodomain and the carboxyl-terminal regions. *The Journal of Biological Chemistry*. 1998;273(12):6763-6768.

24. Itoh N, Yonehara S, Ishii A, et al. The polypeptide encoded by the cDNA for human cell surface antigen Fas can mediate apoptosis. *Cell*. 1991;66:233-243.

25. Boldin MP, Varfolomeev EE, Pancer Z, et al. A novel protein that interacts with the death domain of Fas/APO1 contains a sequence motif related to the death domain. *The Journal of Biological Chemistry*. 1995;270(14):7795-7798.

26. Chinnaiyan AM, O'Rourke K, Tewari M, Dixit VM. FADD, a novel death domain-containing protein, interacts with the death domain of Fas and initiates apoptosis. *Cell*. 1995;81(4):505-512.

27. Hsu H, Xiong J, Goeddel DV. The TNF receptor 1-associated protein TRADD signals cell death and NF-kB activation. *Cell*. 1995;81:495-504.

28. Kischkel FC, Hellbardt S, Behrmann I, et al. Cytotoxicity-dependent APO-1 (Fas/CD95)-associated proteins form a death-inducing signaling complex (DISC) with the receptor. *EMBO Journal*. 1995;14(22):5579-5588.

29. Yang MS, Chan HW, Yu LC. Glutathione peroxidase and glutathione reductase activities are partially responsible for determining the susceptibility of cells to oxidative stress. *Toxicology*. 2006;226:126-130.

30. Medema JP, Scaffidi C, Kischkel FC, et al. FLICE is activated by association with the CD95 death-inducing signaling complex (DISC). *The EMBO Journal*. 1997;16(10):2794-2804.

31. Scarlett JL, Murphy MP. Release of apoptogenic proteins from the mitochondrial intermembrane space during the mitochondrial permeability transition. *FEBS Letters*. 1997;418:282-286.

32. Daugas E, Susin SA, Zamzami N, et al. Mitochondrio-nuclear translocation of AIF in apoptosis and necrosis. *The FASEB Journal*. 2000;14:729-739.

33. Du C, Fang M, Li Y, Li L, Wang X. Smac, a mitochondrial protein that promotes cytochrome c-dependent caspase activation by eliminating IAP inhibition. *Cell*. 2000;102:33-42.

34. Adams JM, Cory S. The Bcl-2 protein family: Arbiters of cell survival. *Science*. 1998;281:1322-1326.

35. Zha H, Aimé-Sempé C, Sato T, Reed JC. Proapoptotic protein Bax heterodimerizes with Bcl-2 and homodimerizes with Bax via a novel domain (BH3) distinct from BH1 and BH2. *The Journal of Biological Chemistry*. 1996;271(13):7440-7444.

36. Boise LH, Gonzalez-Garcia M, Postema CE, et al. bcl-x, a bcl-2-related gene that functions as a dominant regulator of apoptotic cell death. *Cell*. 1993;74:597-606.

37. Eskes R, Desagher S, Antonsson B, Martinou JC. Bid induces the oligomerization and insertion of Bax into the outer mitochondrial membrane. *Molecular and Cellular Biology*. 2000;20(3):929-935.

38. Marzo I, Brenner C, Zamzami N, et al. Bax and Adenine Nucleotide Translocator cooperate in the mitochondrial control of apoptosis. *Science*. 1998;281:2027-2031.

39. Pastorino JG, Chen ST, Tafani M, Snyder JW, Farber JL. The overexpression of Bax produces cell death upon induction of the mitochondrial permeability transition. *The Journal of Biological Chemistry*. 1998;273(13):7770-7775.

40. Oltvai ZN, Korsmeyer SJ. Checkpoints of dueling dimers foil death wishes. *Cell*. 1994;79:189-192.

41. Crompton M. The mitochondrial permeability transition pore and its role in cell death. *The Biochemical Journal*. 1999;341:233-249.

42. Li P, Nijhawan D, Budihardjo I, et al. Cytochrome c and dATP-dependent formation of Apaf-1/caspase-9 complex initiates an apoptotic protease cascade. *Cell*. 1997;91:479-489.

43. Zou H, Henzel WJ, Liu X, Lutschg A, Wang X. Apaf-1, a human protein homologous to C. elegans CED-4, participates in cytochrome c-dependent activation of caspase-3. *Cell*. 1997;90:405-413.

44. Li H, Zhu H, Xu CJ, Yuan J. Cleavage of BID by caspase 8 mediates the mitochondrial damage in the Fas pathway of apoptosis. *Cell*. 1998;94(4):491-501.

45. van Loo G, Schotte P, van Gurp M, et al. Endonuclease G: a mitochondrial protein released in apoptosis and involved in caspase-independent DNA degradation. *Cell Death and Differentiation*. 2001;8:1136-1142.

46. Lorenzo HK, Susin SA, Penninger J, Kroemer G. Apoptosis inducing factor (AIF): a phylogenetically old, caspase-independent effector of cell death. *Cell Death and Differentiation*. 1999;6:516-524.

47. Joza N, Susin SA, Daugas E, et al. Essential role of the mitochondrial apoptosis-inducing factor in programmed cell death. *Nature*. 2001;410:549-554.

48. Susin SA, Lorenzo HK, Zamzami N, et al. Molecular characterization of mitochondrial apoptosis-inducing factor. *Nature*. 1999;397:441-446.

49. Cote J, Ruiz-Carrillo A. Primers for mitochondrial DNA replication generated by endonuclease G. *Science*. 1993;261:765-769.

50. Dargelos E, Brulé C, Stuelsatz P, et al. Up-regulation of calcium-dependent proteolysis in human myoblasts under acute oxidative stress. *Experimental Cell Research*. 2010;316:115-125.

51. Nakagawa T, Yuan J. Cross-talk between two cysteine protease families. Activation of caspase-12 by calpain in apoptosis. *The Journal of Cell Biology*. 2000;150(4):887-894.

52. Cazanave S, Berson A, Haouzi D, et al. High hepatic glutathione stores alleviate Fas-induced apoptosis in mice. *Journal of Hepatology*. 2007;46:858-868.

53. Ghibelli L, Coppola S, Rotilio G, et al. Non-oxidative loss of glutathione in apoptosis via GSH extrusion. *Biochemical and Biophysical Research Communications*. 1995;216(1):313-320.

54. Meier P, Finch A, Evan G. Apoptosis in development. *Nature*. 2000;407:796-801.

55. Alway SE, Siu PM. Nuclear apoptosis contributes to sarcopenia. *Exercise and Sport Sciences Reviews*. 2008;36(2):51-57.

56. Dirks A, Leeuwenburgh C. Apoptosis in skeletal muscle with aging. *American Journal of Physiology: Regulatory, Integrative and Comparative Physiology*. 2002;282:519-527.

57. Allen DL, Linderman JK, Roy RR, et al. Apoptosis: a mechanism contributing to remodeling of skeletal muscle in response to hindlimb unweighting. *American Journal of Physiology: Cell Physiology*. 1997;273:C579-C587.

58. Siu PM, Pistilli EE, Butler DC, Alway SE. Aging influences cellular and molecular responses of apoptosis to skeletal muscle unloading. *American Journal of Physiology: Cell Physiology*. 2005;288:C338-349.

59. Allen DL, Yasui W, Tanaka T, et al. Myonuclear number and myosin heavy chain expression in rat soleus single muscle fibers after spaceflight. *Journal of Applied Physiology*. 1996;81:145-151.

60. Allen DL, Roy RR, Edgerton VR. Myonuclear domains in muscle adaptation and disease. *Muscle & Nerve*. 1999;22:1350–1360.

61. Jejurikar SS, Henkelman EA, Cederna PS, et al. Aging increases the susceptibility of skeletal muscle derived satellite cells to apoptosis. *Experimental Gerontology*. 2006;41:828–836.

62. Koseki T, Inohara N, Chen S, Nunez G. ARC, an inhibitor of apoptosis expressed in skeletal muscle and heart that interacts selectively with caspases. *Proceedings of the National Academy of Sciences USA*. 1998;95:5156-5160.

63. Nagaraju K, Casciola-Rosen L, Rosen A, et al. The inhibition of apoptosis in myositis and in normal muscle cells. *The Journal of Immunology*. 2000;164:5459-5465.

64. Pistilli EE, Jackson JR, Alway SE. Death receptor-associated pro-apoptotic signaling in aged skeletal muscle. *Apoptosis*. 2006;11:2115-2126.

65. Nam Y, Mani K, Ashton AW, et al. Inhibition of both the extrinsic and intrinsic death pathways through nonhomotypic death-fold interactions. *Molecular Cell*. 2004;15:901-912.

66. Gustafsson AB, Tsai JG, Logue SE, Crow MT, Gottlieb RA. Apoptosis repressor with caspase recruitment domain protects against cell death by interfering with Bax activation. *The Journal of Biological Chemistry*. 2004;279(20):21233-21238.

67. Pesce V, Cormio A, Fracasso F, et al. Age-related changes of mitochondrial DNA content and mitochondrial genotypic and phenotypic alterations in rat hind-limb skeletal muscles. *The Journals of Gerontology. Series A, Biological Sciences and Medical Sciences*. 2005;60A(6):715-723.

68. Pette D, Staron RS. Myosin isoforms, muscle fiber types, and transitions. *Microscopy Research and Technique*. 2000;50:500-509.

69. Berchtold MW, Brinkmeier H, Muntener M. Calcium ion in skeletal muscle: Its crucial role for muscle function, plasticity, and disease. *Physiological Reviews*. 2000;80(3):1215-1265.

70. Quadrilatero J, Bombardier E, Norris SM, et al. Prolonged moderate intensity aerobic exercise does not alter apoptotic signaling and DNA fragmentation in human skeletal muscle. *American Journal of Physiology: Endocrinology and Metabolism*. 2009;298:E534-547.

71. Leeuwenburgh C, Gurley CM, Strotman BA, Dupont-Versteegden EE. Age-related differences in apoptosis with disuse atrophy in soleus muscle. *American Journal of Physiology: Regulatory, Integrative and Comparative Physiology*. 2005;288:R1288-R1296.

72. Phillips T, Leeuwenburgh C. Muscle fiber-specific apoptosis and TNF-α signaling in sarcopenia are attenuated by life-long calorie restriction. *The FASEB Journal*. 2005;19(6):668-670.

73. Rice KM, Blough ER. Sarcopenia-related apoptosis is regulated differently in fast and slow-twitch muscles of the aging F344/N x BN rat model. *Mechanisms of Ageing and Development*. 2006;127:670-679.

74. Finkel T, Holbrook NJ. Oxidants, oxidative stress and the biology of ageing. *Nature*. 2000;408:239-247.

75. Chandra J, Samali A, Orrenius S. Triggering and modulation of apoptosis by oxidative stress. *Free Radical Biology & Medicine*. 2000;29(3/4):323–333.

76. Pansarasa O, Bertorelli L, Vecchiet J, Felzani G, Marzatico F. Age-dependent changes of antioxidant activities and markers of free radical damage in human skeletal muscle. *Free Radical Biology & Medicine*. 1999;27(5/6):617- 622.

77. Parise G, Kaczor JJ, Mahoney DJ, Phillips SM, Tarnopolsky MA. Oxidative stress and the mitochondrial theory of aging in human skeletal muscle. *Experimental Gerontology*. 2004;39:1391-1400.

78. Pansarasa O, Felzani G, Vecchiet J, Marzatico F. Antioxidant pathways in human aged skeletal muscle: relationship with the distribution of type II fibers. *Experimental Gerontology*. 2002;37:1069-1075.

79. Gomez-Cabrera M, Borrás C, Pallardó FV, et al. Decreasing xanthine oxidase-mediated oxidative stress prevents useful cellular adaptations to exercise in rats. *The Journal of Physiology*. 2005;567(1):113-120.

80. Kang C, O'Moore KM, Dickman JR, Ji LL. Exercise activation of muscle peroxisome proliferator-activated receptor-gamma coactivator-1alpha signaling is redox sensitive. *Free Radical Biology & Medicine*. 2009;47:1394-1400.

81. Archuleta TL, Lemieux AM, Saengsirisuwan V, et al. Oxidant stress-induced loss of IRS-1 and IRS-2 proteins in rat skeletal muscle: role of p38 MAPK. *Free Radical Biology & Medicine*. 2009;47:1486-1493.

82. Leeuwenburgh C, Leichtweis S, Hollander J, et al. Effect of acute exercise on glutathione deficient heart. *Molecular and Cellular Biochemistry*. 1996;156:17-24.

83. McCutchan HJ, Schwappach JR, Enquist EG, et al. Xanthine oxidase-derived H2O2 contributes to reperfusion injury of ischemic skeletal muscle. *American Journal of Physiology: Heart and Circulatory Physiology*. 1990;258:H1415-H1419.

84. Messina S, Altavilla D, Aguennouz M, et al. Lipid peroxidation inhibition blunts nuclear factor- kappaB activation, reduces skeletal muscle degeneration, and enhances muscle function in mdx mice. *American Journal Of Pathology*. 2006;168(3):918-926.

85. Whitehead NP, Pham C, Gervasio OL, Allen DG. N-Acetylcysteine ameliorates skeletal muscle pathophysiology in mdx mice. *The Journal of Physiology*. 2008;586(7):2003-2014.

86. Cadenas E, Davies KJ. Mitochondrial free radical generation, oxidative stress and aging. *Free Radical Biology & Medicine*. 2000;29(3/4):222-230.

87. Miquel J, Economos AC, Fleming J, Johnson JE. Mitochondrial role in cell aging. *Experimental Gerontology*. 1980;15:575-591.

88. Zhao K, Zhao G, Wu D, et al. Cell-permeable peptide antioxidants targeted to inner mitochondrial membrane inhibit mitochondrial swelling, oxidative cell death, and reperfusion injury. *The Journal of Biological Chemistry*. 2004;279(33):34682-34690.

89. Tahara EB, Navarete FD, Kowaltowski AJ. Tissue-, substrate-, and site-specific characteristics of mitochondrial reactive oxygen species generation. *Free Radical Biology & Medicine*. 2009;46:1283-1297.

90. Apple FS, Hyde JE, Ingersoll-Stroubos AM, Theologides A. Geographic distribution of xanthine oxidase, free radical scavengers, creatine kinase, and lactate dehydrogenase enzyme

systems in rat heart and skeletal muscle. *The American Journal of Anatomy*. 1991;192:319-323.

91. Judge AR, Dodd SL. Xanthine oxidase and activated neutrophils cause oxidative damage to skeletal muscle after contractile claudication. *American Journal of Physiology: Heart and Circulatory Physiology*. 2004;286:H252-H256.

92. Kondo H, Nakagaki I, Sasaki S, Hori S, Itokawa Y. Mechanism of oxidative stress in skeletal muscle atrophied by immobilization. *The American Journal of Physiology: Endocrinology and Metabolism*. 1993;265:E839-E844.

93. Espinosa A, Leiva A, Pena M, et al. Myotube depolarization generates reactive oxygen species through NAD(P)H Oxidase; ROS-elicited Ca 2+ stimulates ERK, CREB, early genes. *Journal of Cellular Physiology*. 2006;209:379-388.

94. Hidalgo C, Sánchez G, Barrientos G, Aracena-Parks P. A transverse tubule NADPH oxidase activity stimulates calcium release from isolated triads via ryanodine receptor type 1 S-glutathionylation. *The Journal of Biological Chemistry*. 2006;281(36):26473-26482.

95. Wei Y, Sowers JR, Clark SE, et al. Angiotensin II-induced skeletal muscle insulin resistance mediated by NF-kappaB activation via NADPH oxidase. *American Journal of Physiology: Endocrinology and Metabolism*. 2008;294:E345-E351.

96. Xia R, Webb JA, Gnall LL, Cutler K, Abramson JJ. Skeletal muscle sarcoplasmic reticulum contains a NADH-dependent oxidase that generates superoxide. *American Journal of Physiology: Cell Physiology*. 2003;285:C215-221.

97. Sato T, Machida T, Takahashi S, et al. Fas-mediated apopotosome formation is dependent on reactive oxygen species derived from mitochondrial permeability transition in Jurkat cells. *The Journal of Immunology*. 2004;173:285-296.

98. Siu PM, Wang Y, Alway SE. Apoptotic signaling induced by H2O2-mediated oxidative stress in differentiated C2C12 myotubes. *Life Sciences*. 2009;84:468-481.

99. Nam Y, Mani K, Wu L, et al. The apoptosis inhibitor ARC undergoes ubiquitin-proteasomal-mediated degradation in response to death stimuli: identification of a degradation-resistant mutant. *The Journal of Biological Chemistry*. 2007;282(8):5522-5528.

100. Neuss M, Monticone R, Lundberg MS, et al. The apoptotic regulatory protein ARC (apoptosis repressor with caspase recruitment domain) prevents oxidant stress-mediated cell death by preserving mitochondrial function. *The Journal of Biological Chemistry*. 2001;276(36):33915-33922.

101. Haynes RL, Brune B, Townsend AJ. Apoptosis in RAW 264.7 cells exposed to 4-hydroxy-2-nonenal: dependence on cytochrome c release but not p53 accumulation. *Free Radical Biology & Medicine*. 2001;30(8):884-894.

102. Kutuk O, Adli M, Poli G, Basaga H. Resveratrol protects against 4-HNE induced oxidative stress and apoptosis in Swiss 3T3 fibroblasts. *BioFactors*. 2004;20:1-10.

103. Van Remmen H, Williams MD, Guo Z, et al. Knockout mice heterozygous for Sod2 show alterations in cardiac mitochondrial function and apoptosis. *American Journal of Physiology: Heart and Circulatory Physiology*. 2001;281:H1422-H1432.

104. Reddy VN, Kasahara E, Hiraoka M, Lin L, Ho Y. Effects of variation in superoxide dismutases (SOD) on oxidative stress and apoptosis in lens epithelium. *Experimental Eye Research*. 2004;79:859-868.

105. Schriner SE, Linford NJ, Martin GM, et al. Extension of murine life span by overexpression of catalase targeted to mitochondria. *Science*. 2005;308:1909-1911.

106. Tome ME, Baker AF, Powis G, Payne CM, Briehl MM. Catalase-overexpressing thymocytes are resistant to glucocorticoid-induced apoptosis and exhibit increased net tumor growth. *Cancer Research*. 2001;61:2766 -2773.

107. Bejma J, Ji LL. Aging and acute exercise enhance free radical generation in rat skeletal muscle. *Journal of Applied Physiology*. 1999;87(1):465-470.

108. Chabi B, Ljubicic V, Menzies KJ, et al. Mitochondrial function and apoptotic susceptibility in aging skeletal muscle. *Aging Cell*. 2008;7:2–12.

109. Figueiredo PA, Powers SK, Ferreira RM, Appell HJ, Duarte JA. Aging impairs skeletal muscle mitochondrial bioenergetic function. *The Journals of Gerontology. Series A, Biological Sciences and Medical Sciences*. 2009;64A(1):21-33.

110. Jang YC, Lustgarten MS, Liu Y, et al. Increased superoxide in vivo accelerates age-associated muscle atrophy through mitochondrial dysfunction and neuromuscular junction degeneration. *The FASEB Journal*. 2009;24:1376-1390.

111. Marzani B, Felzani G, Bellomo RG, Vecchiet J, Marzatico F. Human muscle aging: ROS-mediated alterations in rectus abdominis and vastus lateralis muscles. *Experimental Gerontology*. 2005;40:959-965.

112. Evans WJ. What is sarcopenia? *The Journals of Gerontology Series A*. 1995;50A:5-8.

113. Greiwe JS, Cheng B, Rubin DC, Yarasheski KE, Semenkovich CF. Resistance exercise decreases skeletal muscle tumor necrosis factor alpha in frail elderly humans. *The FASEB Journal*. 2001;15:475-482.

114. Riva C, Chevrier C, Pasqual N, Saks V, Rossi A. Bcl-2/Bax protein expression in heart, slow-twitch and fast-twitch muscles in young rats growing under chronic hypoxia conditions. *Molecular and Cellular Biochemistry*. 2001;226:9-16.

115. Ames BN, Shigenaga MK, Hagen TM. Oxidants, antioxidants, and the degenerative diseases of aging. *Proceedings of the National Academy of Sciences USA*. 1993;90:7915-7922.

116. Anderson EJ, Neufer PD. Type II skeletal myofibers possess unique properties that potentiate mitochondrial H2O2 generation. *American Journal of Physiology: Cell Physiology*. 2006;290:C844-C851.

117. Halliwell B. Reactive species and antioxidants. Redox biology is a fundamental theme of aerobic life. *Plant Physiology*. 2006;141:312-322.

118. Mandeles S, Bloch K. Enzymatic synthesis of gamma-glutamylcysteine. *The Journal of Biological Chemistry*. 1954:639-646.

119. Snoke JE, Yanari S, Bloch K. Synthesis of glutathione from gamma-glutamylcysteine. *The Journal of Biological Chemistry*. 1952:573-598.

120. Mills GC. Hemoglobin catabolism: Glutathione peroxidase, an erythrocyte enzyme which protects hemoglobin from oxidative breakdown. *The Journal of Biological Chemistry*. 1957:189-197.

121. Lopez-Barea J, Lee C. Mouse-liver glutathione reductase: Purification, kinetics, and regulation. *European Journal of Biochemistry*. 1979;98:487-499.

122. Meister A. Glutathione-ascorbic acid antioxidant system in animals. *The Journal of Biological Chemistry*. 1994;269(13):9397-9400.

123. Martensson J, Meister A. Glutathione deficiency decreases tissue ascorbate levels in newborn rats: Ascorbate spares glutathione and protects. *Proceedings of the National Academy of Sciences USA*. 1991;88:4656-4660.

124. Maiorino M, Coassin M, Roveri A, Ursini F. Microsomal lipid peroxidation: Effect of vitamin E and its functional interaction with phospholipid hydroperoxide glutathione peroxidase. *Lipids*. 1989;24:721-726.

125. Pompella A, Visvikis A, Paolicchi A, De Tata V, Casini AF. The changing faces of glutathione, a cellular protagonist. *Biochemical Pharmacology*. 2003;66:1499–1503.

126. Bojes HK, Datta K, Xu J, et al. Bcl-xL overexpression attenuates glutathione depletion in FL5.12 cells following interleukin-3 withdrawal. *The Biochemical Journal*. 1997;325:315-319.

127. Dalton TP, Chen Y, Schneider SN, Nebert DW, Shertzer HG. Genetically altered mice to evaluate glutathione homeostasis in health and disease. *Free Radical Biology & Medicine*. 2004;37(10):1511-1526.

128. Friesen C, Kiess Y, Debatin K. A critical role of glutathione in determining apoptosis sensitivity and resistance in leukemia cells. *Cell Death and Differentiation*. 2004;11:S73-85.

129. Ghibelli L, Coppola S, Fanelli C, et al. Glutathione depletion causes cytochromec release even in the absence of cell commitment to apoptosis. *The FASEB Journal*. 1999;13:2031-2036.

130. Haouzi D, Lekehal M, Tinel M, et al. Prolonged, but not acute, glutathione depletion promotes Fas-mediated mitochondrial permeability transition and apoptosis in mice. *Hepatology*. 2001;33:1181-1188.

131. Khamaisi M, Kavel O, Rosenstock M, et al. Effect of inhibition of glutathione synthesis on insulin action: in vivo and in vitro studies using buthionine sulfoximine. *The Biochemical Journal*. 2000;349:579-586.

132. Leeuwenburgh C, Ji LL. Glutathione depletion in rested and exercised mice: biochemical consequence and adaptation. *Archives of Biochemistry and Biophysics*. 1995;316(2):941-949.

133. Magalhães J, Ascensão A, Soares JM, et al. Acute and severe hypobaric hypoxia-induced muscle oxidative stress in mice: the role of glutathione against oxidative damage. *European Journal of Applied Physiology*. 2004;91:185-191.

134. Martensson J, Meister A. Mitochondrial damage in muscle occurs after marked depletion of glutathione and is prevented by giving glutathione monoester. *Proceedings of the National Academy of Sciences*. 1989;86:471-475.

135. Nagai H, Matsumaru K, Feng G, Kaplowitz N. Reduced glutathione depletion causes necrosis and sensitization to tumor necrosis factor-alpha-induced apoptosis in cultured mouse hepatocytes. *Hepatology*. 2002;36:55-64.

136. Reliene R, Schiestl RH. Glutathione depletion by buthionine sulfoximine induces DNA deletions in mice. *Carcinogenesis*. 2006;27(2):240-244.

137. Sen CK, Atalay M, Hanninen O. Exercise-induced oxidative stress: glutathione supplementation and deficiency. *Journal of Applied Physiology*. 1994;77(5):2177-2187.

138. Tupling AR, Vigna C, Ford RJ, et al. Effects of buthionine sulfoximine treatment on diaphragm contractility and SR Ca2+ pump function in rats. *Journal of Applied Physiology*. 2007;103:1921-1928.

139. Watanabe T, Sagisaka H, Arakawa S, et al. A novel model of continuous depletion of glutathione in mice treated with L-buthionine (S,R)-sulfoximine. *The Journal of Toxicological Sciences*. 2003;28(5):455-469.

140. Griffith OW, Meister A. Glutathione: Interorgan translocation, turnover, and metabolism. *Proceedings of the National Academy of Sciences USA*. 1979;76(11):5606-5610.

141. Jain A, Mårtensson J, Stole E, Auld PA, Meister A. Glutathione deficiency leads to mitochondrial damage in brain. *Proceedings of the National Academy of Sciences USA*. 1991;88:1913-1917.

142. Coppola S, Ghibelli L. GSH extrusion and and the mitochondrial pathway of apoptotic signalling. *Biochemical Society Transactions*. 2000;28(2):56-61.

143. Hammond CL, Madejczyk MS, Ballatori N. Activation of plasma membrane reduced glutathione transport in death receptor apoptosis of HepG2 cells. *Toxicology and Applied Pharmacology*. 2004;195:12-22.

144. van Den Dobbelsteen DJ, Nobel CS, Schlegel J, et al. Rapid and specific efflux of reduced glutathione during apoptosis induced by anti-Fas/ APO-1 antibody. *The Journal of Biological Chemistry*. 1996;271:15420-15427.

145. Franklin CC, Krejsa CM, Pierce RH, et al. Caspase-3-dependent cleavage of the glutamate-L-cysteine ligase catalytic subunit during apoptotic dell Death. *American Journal of Pathology*. 2002;160(5):1887-1894.

146. Macho A, Hirsch T, Marzo I, et al. Glutathione depletion is an early and calcium elevation is a late event of thymocyte apoptosis. *The Journal of Immunology*. 1997;158:4612-4619.

147. Marchetti P, Castedo M, Susin SA, et al. Mitochondrial permeability transition is a central coordinating event of apoptosis. *Journal of Experimental Medicine*. 1996;184:1155-1160.

148. Meredith MJ, Cusick CL, Soltaninassab S, et al. Expression of Bcl-2 increases intracellular glutathione by inhibiting methionine-dependent GSH efflux. *Biochemical and Biophyical Research Communications*. 1998;248:458-463.

149. Kane DJ, Sarafian TA, Anton R, et al. Bcl-2 inhibition of neural death: Decreased generation of reactive oxygen species. *Science*. 1993;262(5137):1274-1277.

150. Mirkovic N, Voehringer DW, Story MD, et al. Resistance to radiation-induced apoptosis in Bcl-2-expressing cells is reversed by depleting cellular thiols. *Oncogene*. 1997;15:1461-1470.

151. Voehringer DW, McConkey DJ, McDonnell TJ, Brisbay S, Meyn RE. Bcl-2 expression causes redistribution of glutathione to the nucleus. *Proceedings of the National Academy of Sciences USA*. 1998;95:2956-2960.

152. Armstrong JS, Steinhauer KK, Hornung B, et al. Role of glutathione depletion and reactive oxygen species generation in apoptotic signaling in a human B lymphoma cell line. *Cell Death and Differentiation*. 2002;9:252-263.

153. Armstrong JS, Jones DP. Glutathione depletion enforces the mitochondrial permeability transition and causes cell death in HL60 cells that overexpress Bcl-2. *The FASEB Journal*. 2002;16(10).

154. Valverde M, Rojas E, Kala SV, Kala G, Lieberman MW. Survival and cell death in cells constitutively unable to synthesize glutathione. *Mutation Research*. 2006;594:172-180.

155. Lewis-Wambi JS, Kim HR, Wambi C, et al. Buthionine sulfoximine sensitizes antihormone-resistant human breast cancer cells to estrogen-induced apoptosis. *Breast Cancer Research*. 2008;10(6).

156. Déas O, Dumont C, Mollereau B, et al. Thiol-mediated inhibition of FAS and CD2 apoptotic signaling in activated human peripheral T cells. *International Immunology*. 1997;9(1):117-125.

157. Reed DJ, Babson JR, Beatty PW, et al. High-performance liquid chromatography analysis of nanomole levels of glutathione, glutathione disulfide, and related thiols and disulfides. *Analytical Biochemistry*. 1980;106:55-62.

158. Braga M, Hikim AP, Datta S, et al. Involvement of oxidative stress and caspase 2-mediated intrinsic pathway signaling in age-related increase in muscle cell apoptosis in mice. *Apoptosis*. 2008;13:822-832.

159. Ford RJ, Graham DA, Denniss SG, Quadrilatero J, Rush JW. Glutathione depletion in vivo enhances contraction and attenuates endothelium-dependent relaxation of isolated rat aorta. *Free Radical Biology & Medicine*. 2006;40(4):670-8.

160. Griffith OW, Meister A. Potent and specific inhibition of glutathione synthesis by Buthionine Sulfoximine (S-n-Butyl Homocysteine Sulfoximine). *The Journal of Biological Chemistry*. 1979;254(16):7558-7560.

161. Rajasekaran NS, Devaraj NS, Devaraj H. Modulation of rat erythrocyte antioxidant defense system by buthionine sulfoximine and its reversal by glutathione monoester therapy. *Biochimica et Biophysica Acta*. 2004;1688:121-129.

162. Sies H, Akerboom TP. Glutathione disulfide (GSSG) efflux from cells and tissues. *Methods in Enzymology*. 1984;105:445-451.

163. Rebrin I, Sohal RS. Pro-oxidant shift in glutathione redox state during aging. *Advanced Drug Delivery Reviews*. 2008;60:1545-1552.

164. Michael B, Yano B, Sellers RS, et al. Evaluation of organ weights for rodent and non-rodent toxicity studies: a review of regulatory guidelines and a survey of current practices. *Toxicologic Pathology*. 2007;35:742-750.

165. Cattan V, Mercier N, Gardner JP, et al. Chronic oxidative stress induces a tissue-specific reduction in telomere length in CAST/Ei mice. *Free Radical Biology & Medicine*. 2008;44:1592-1598.

166. Vaziri ND, Wang XQ, Oveisi F, Rad B. Induction of oxidative stress by glutathione depletion causes severe hypertension in normal rats. *Hypertension*. 2000;36:142-146.

167. Coggan AR, Spina RJ, King DS, et al. Histochemical and enzymatic comparison of the gastrocnemius muscle of young and elderly men and women. *Journal of Gerontology*. 1992;47(3):B71-76.

168. Hutchison DL, Roy RR, Hodgson JA, Edgerton VR. EMG amplitude relationships between the rat soleus and medial gastrocnemius during various motor tasks. *Brain Research*. 1989;502:233-244.

169. Schmuck G, Röhrdanz E, Tran-Thi QH, Kahl R, Schlüter G. Oxidative stress in rat cortical neurons and astrocytes induced by paraquat in vitro. *Neurotoxicity Research*. 2002;4(1):1-13.

170. Jones DP, Eklow L, Thor H, Orrenius S. Metabolism of hydrogen peroxide in isolated hepatocytes: Relative contributions of catalase and glutathione peroxidase in decomposition of endogenously generated H2O2. *Archives of Biochemistry and Biophysics*. 1981;210(2):505-516.

171. Ji LL, Dillon D, Wu E. Alteration of antioxidant enzymes with aging in rat skeletal muscle and liver. *The American Journal of Physiology: Regulatory, Integrative and Comparative Physiology*. 1990;258:918-923.

172. Suwa M, Egashira T, Nakano H, Sasaki H, Kumagai S. Metformin increases the PGC-1alpha protein and oxidative enzyme activities possibly via AMPK phosphorylation in skeletal muscle in vivo. *Journal of Applied Physiology*. 2006;101:1685-92.

173. Armstrong RB, Phelps RO. Muscle fiber type composition of the rat hindlimb. *The American Journal of Anatomy*. 1984;171:259-272.

174. Delp MD, Duan C. Composition and size of type I, IIA, IID/X, and IIB fibers and citrate synthase activity of rat muscle. *Journal of Applied Physiology*. 1996;80(1):261-270.

175. Çakatay U, Telci A, Kayali R, Ackay T, Sivas A. Relation of aging with oxidative protein damage parameters in the rat skeletal muscle. *Clinical Biochemistry*. 2003;36:51-55.

176. Uchida K. 4-Hydroxy-2-nonenal: a product and mediator of oxidative stress. *Progress in Lipid Research*. 2003;42(4):318-343.

177. Awasthi YC, Sharma R, Sharma A, et al. Self-regulatory role of 4-hydroxynonenal in signaling for stress-induced programmed cell death. *Free Radical Biology & Medicine*. 2008;45:111-118.

178. Awasthi YC, Yang Y, Tiwari NK, et al. Regulation of 4-hydroxynonenal-mediated signaling by glutathione S-transferases. *Free Radical Biology & Medicine*. 2004;37(5):607-619.

179. Leeuwenburgh C, Fiebig R, Chandwaney R, Ji LL. Aging and exercise training in skeletal muscle : responses of glutathione and antioxidant enzyme. *American Journal of Physiology: Regulatory, Integrative and Comparative Physiology*. 1994;267:439-445.

180. Lawler JM, Powers SK, Visser T, et al. Acute exercise and skeletal muscle antioxidant and metabolic enzymes: effects of fiber type and age. *The American Journal of Physiology: Regulatory, Integrative and Comparative Physiology*. 1993;265:R1344-1350.

181. Smith HK, Maxwell L, Martyn JA, Bass JJ. Nuclear DNA fragmentation and morphological alterations in adult rabbit skeletal muscle after short-term immobilization. *Cell and Tissue Research*. 2000;302:235-241.

182. Dirks AJ, Leeuwenburgh C. Aging and lifelong calorie restriction result in adaptations of skeletal muscle apoptosis repressor, apoptosis-inducing factor, X-linked inhibitor of apoptosis, caspase-3, and caspase-12. *Free Radical Biology & Medicine*. 2004;36(1):27-39.

183. Marzetti E, Wohlgemuth SE, Lees HA, et al. Age-related activation of mitochondrial caspase-independent apoptotic signaling in rat gastrocnemius muscle. *Mechanisms of Ageing and Development*. 2008;129:542-549.

184. Bruusgaard JC, Gundersen K. In vivo time-lapse microscopy reveals no loss of murine myonuclei during weeks of muscle atrophy. *The Journal of Clinical Investigation*. 2008;118(4):1450.

185. Mitch WE, Goldberg AL. Mechanisms of muscle wasting: The role of the ubiquitin-proteasome pathway. *The New England Journal of Medicine*. 1996;335(25):1897-1905.

186. Tawa NE, Odessey R, Goldberg AL. Inhibitors of the proteasome reduce the accelerated proteolysis in atrophying rat skeletal muscles. *The Journal of Clinical Investigation*. 1997;100(1):197-203.

187. Balagopal P, Rooyackers OE, Adey DB, Ades PA, Nair KS. Effects of aging on in vivo synthesis of skeletal muscle myosin heavy-chain and sarcoplasmic protein in humans. *The American Journal of Physiology*. 1997;273:E790-800.

188. Siu PM, Pistilli EE, Alway SE. Apoptotic responses to hindlimb suspension in gastrocnemius muscles from young adult and aged rats. *American Journal of Physiology. Regulatory, Integrative and Comparative Physiology*. 2005;289:R1015-1026.

189. Larsen BD, Rampalli S, Burns LE, et al. Caspase 3/caspase-activated DNase promote cell differentiation by inducing DNA strand breaks. *Proceedings of the National Academy of Sciences USA*. 2010;107(9):4230-4235.

190. Freer-Prokop M, O'Flaherty J, Ross JA, Weyman CM. Non-canonical role for the TRAIL receptor DR5/FADD/caspase pathway in the regulation of MyoD expression and skeletal myoblast differentiation. *Differentiation*. 2009;78:205-212.

191. Snow MH. An autoradiographic study of satellite cell differentiation into regenerating myotubes following transplantation of muscles in young rats. *Cell and Tissue Research*. 1978;186:535-540.

192. Siu PM, Alway SE. Mitochondria-associated apoptotic signalling in denervated rat skeletal muscle. *The Journal of Physiology*. 2005;565(1):309-323.

193. Chung L, Ng Y. Age-related alterations in expression of apoptosis regulatory proteins and heat shock proteins in rat skeletal muscle. *Biochimica et Biophysica Acta*. 2006;1762:103-109.

194. Saleh A, Srinivasula SM, Balkir L, Robbins PD, Alnemri ES. Negative regulation of the Apaf-1 apoptosome by Hsp70. *Nature Cell Biology*. 2000;2:476-483.

195. Jäättelä M, Wissing D, Kokholm K, Kallunki T, Egeblad M. Hsp70 exerts its anti-apoptotic function downstream of caspase-3-like proteases. *The EMBO journal*. 1998;17(21):6124-6134.

196. Galluzzi L, Joza N, Tasdemir E, et al. No death without life: Vital functions of apoptotic effectors. *Cell Death and Differentiation*. 2008;15(7):1113-1123.

197. Conley KE, Jubrias SA, Esselman PC. Oxidative capacity and ageing in human muscle. *The Journal of Physiology*. 2000;526(1):203-210.

198. Short KR, Bigelow ML, Kahl J, et al. Decline in skeletal muscle mitochondrial function with aging in humans. *Proceedings of the National Academy of Sciences of the United States of America*. 2005;102(15):5618-5623.

199. Siu PM, Alway SE. Aging alters the reduction of pro-apoptotic signaling in response to loading-induced hypertrophy. *Experimental Gerontology*. 2006;41:175-188.

200. Rivero JL, Talmadge RJ, Edgerton VR. Fibre size and metabolic properties of myosin heavy chain-based fibre types in rat skeletal muscle. *Journal of Muscle Research and Cell Motility*. 1998;19:733-742.

201. Ji L, Fu R, Mitchell E. Glutathione and antioxidant enzymes in skeletal muscle: effects of fiber type and exercise intensity. *Journal of Applied Physiology*. 1992;73:1854-1859.

202. Locke M, Noble EG, Atkinson BG. Inducible isoform of HSP70 is constitutively expressed in a muscle fiber type specific pattern. *American Journal of Physiology: Cell Physiology*. 1991;261:C774-779.

203. Garlick PJ, Maltin CA, Baillie AG, Delday MI, Grubb DA. Fiber-type composition of nine rat muscles. II Relationship to protein turnover. *The American Journal of Physiology*. 1989;257(6 Pt 1):E828-32.

204. Gibson ME, Schultz E. The distribution of satellite cells and their relationship to specific fiber types in soleus and extensor digitorum longus muscles. *Anatomical Record*. 1982;202:329-337.